JVI Journals.ASM.org

Host and Viral Determinants of Mx2 Antiretroviral Activity

Idoia Busnadiego,[a] Melissa Kane,[b,c] Suzannah J. Rihn,[b,c] Hannah F. Preugschas,[a] Joseph Hughes,[a] Daniel Blanco-Melo,[b,c] Victoria P. Strouvelle,[a] Trinity M. Zang,[b,c,d] Brian J. Willett,[a] Chris Boutell,[a] Paul D. Bieniasz,[b,c,d] Sam J. Wilson[a]

MRC–University of Glasgow Centre for Virus Research, Institute of Infection, Inflammation and Immunity, University of Glasgow, Glasgow, United Kingdom[a]; Aaron Diamond AIDS Research Center, The Rockefeller University, New York, New York, USA[b]; Laboratory of Retrovirology, The Rockefeller University, New York, New York, USA[c]; Howard Hughes Medical Institute, Aaron Diamond AIDS Research Center, New York, New York, USA[d]

ABSTRACT

Myxovirus resistance 2 (Mx2/MxB) has recently been uncovered as an effector of the anti-HIV-1 activity of type I interferons (IFNs) that inhibits HIV-1 at an early stage postinfection, after reverse transcription but prior to proviral integration into host DNA. The mechanistic details of Mx2 antiviral activity are not yet understood, but a few substitutions in the HIV-1 capsid have been shown to confer resistance to Mx2. Through a combination of *in vitro* evolution and unbiased mutagenesis, we further map the determinants of sensitivity to Mx2 and reveal that multiple capsid (CA) surfaces define sensitivity to Mx2. Intriguingly, we reveal an unanticipated sensitivity determinant within the C-terminal domain of capsid. We also report that Mx2s derived from multiple primate species share the capacity to potently inhibit HIV-1, whereas selected nonprimate orthologs have no such activity. Like TRIM5α, another CA targeting antiretroviral protein, primate Mx2s exhibit species-dependent variation in antiviral specificity against at least one extant virus and multiple HIV-1 capsid mutants. Using a combination of chimeric Mx2 proteins and evolution-guided approaches, we reveal that a single residue close to the N terminus that has evolved under positive selection can determine antiviral specificity. Thus, the variable N-terminal region can define the spectrum of viruses inhibited by Mx2.

IMPORTANCE

Type I interferons (IFNs) inhibit the replication of most mammalian viruses. IFN stimulation upregulates hundreds of different IFN-stimulated genes (ISGs), but it is often unclear which ISGs are responsible for inhibition of a given virus. Recently, Mx2 was identified as an ISG that contributes to the inhibition of HIV-1 replication by type I IFN. Thus, Mx2 might inhibit HIV-1 replication in patients, and this inhibitory action might have therapeutic potential. The mechanistic details of how Mx2 inhibits HIV-1 are currently unclear, but the HIV-1 capsid protein is the likely viral target. Here, we determine the regions of capsid that specify sensitivity to Mx2. We demonstrate that Mx2 from multiple primates can inhibit HIV-1, whereas Mx2 from other mammals (dogs and sheep) cannot. We also show that primate variants of Mx2 differ in the spectrum of lentiviruses they inhibit and that a single residue in Mx2 can determine this antiviral specificity.

HIV-1 is a chronic infection that persists despite the concerted action of the innate and acquired immune responses. A key component of innate immunity is the interferon (IFN) response and HIV-1 replication is substantially inhibited by type I IFNs both *in vitro* (1) and *in vivo* (2). A number of IFN-stimulated genes (ISGs) such as APOBEC3G, TRIM5α, and tetherin have been reported to attenuate retroviral replication *in vivo* (3–5), and SAMHD1 is likely to be similarly important in this regard (6, 7). However, these factors are all either evaded in their natural hosts or antagonized by viral accessory genes (8, 9). Numerous other ISGs, such as CNP, ZAP, and MOV10, have been reported to inhibit HIV-1 replication *in vitro* (10–12). However, none of these factors are likely responsible for the strong IFN-mediated inhibition of HIV-1 infection observed in most human primary cells and some cell lines, particularly during the early steps of the replication cycle (6, 7, 10–13).

Myxovirus resistance (Mx) proteins are a family of dynamin-like GTPases first identified for their ability to confer resistance to lethal doses of influenza A virus (14, 15). Most mammals encode two paralogous Mx proteins, Mx1 and Mx2 (sometimes referred to as MxA and MxB). The Mx1 proteins have been reported to exhibit activity against viruses from a variety of families, while the Mx2 lineage was previously thought to be limited to cellular functions (16), despite being strongly induced by IFN. Recently, we (and others) found that Mx2 is capable of efficiently inhibiting the early steps of HIV-1 infection *in vitro* (17–20). Mx2 could therefore contribute to the IFN-mediated suppression of HIV-1 replication that is observed *in vivo* (2). Mx2 impedes the early steps of HIV-1 infection prior to chromosomal integration of proviral DNA (18–20), perhaps by inhibiting nuclear import of HIV-1 DNA following reverse transcription (18, 19). The mechanistic details of how inhibition occurs are currently unclear. However, the capsid (CA) region of *gag* is a major determinant of Mx2 sensitivity, and a few single-amino-acid substitutions in CA have been reported to confer partial or complete escape from Mx2 activity (18–20). Notably, host cyclophilins could be involved in Mx2 antiviral activity since several substitutions in the cyclophilin binding loop, including at the cyclophilin binding site, enable escape from Mx2 (18–20). An interaction with host cyclophilins has been proposed as a requirement for Mx2 inhibition due to the

Received 23 January 2014 **Accepted** 15 April 2014
Published ahead of print 23 April 2014
Editor: B. H. Hahn
Address correspondence to Paul D. Bieniasz, pbienias@adarc.org, or Sam J. Wilson, sam.wilson@glasgow.ac.uk.

doi:10.1128/JVI.00214-14

ability of cyclosporine to rescue infection in the presence of Mx2 (20).

Examining the spectrum of retroviruses inhibited by species variants of restriction factors has previously been of great value in uncovering the molecular details of antiretroviral activity. Because orthologous variants often inhibit different spectra of retroviruses, these analyses can define the determinants of viral sensitivity to, and host specificity of, antiviral activity. Here, we show that several, but not all, mammalian variants of Mx2 exhibit antilentiviral activity. Upon examining a panel of retroviruses, we noted that Mx2 antiviral specificity is largely confined to primate lentiviruses and that Mason-Pfizer monkey virus (MPMV), a betaretrovirus, is also partially sensitive to Mx2. In addition, using *in vitro* evolution and unbiased mutagenesis, we found that multiple localized substitutions in the C-terminal domain of CA can confer resistance to Mx2. Intriguingly, primate Mx2 variants exhibit species-dependent activity against O-group HIV-1 and some M-group HIV-1 CA mutants, indicating that divergent Mx2s have divergent antiretroviral specificities. Using chimeric Mx2 proteins and evolution-guided approaches, we demonstrate that a single residue close to the N terminus of Mx2 that has evolved under positive selection can determine this antiviral specificity.

MATERIALS AND METHODS

Mx2 sequences and plasmid construction. The species variants of Mx2 were cloned from the following cell lines: FrHK4 (*Macaca mulatta* NM_001079696.1), Vero (*Chlorocebus aethiops* [Vervet], KF925356), CPT-Tert (*Ovis aries*, KF925355), and MDCK (*Canis lupus familiaris*, XM_005638734.1). The cloning of human Mx2 was described previously (18). The different cell lines were stimulated overnight with 1,000 U of peginterferon alfa-2b/ml and total RNA was extracted using TRIzol (Life Technologies) in accordance with the manufacturer's instructions. This RNA was used as a template to generate cDNA (Superscript III; Life Technologies) in accordance with the manufacturer's instructions. Species variants of Mx2 were PCR amplified using a high-fidelity polymerase prior to insertion in the N-terminal myc-tagged doxycycline-inducible lentiviral vectors (LKO derivatives) using SfiI. Because no AGM Mx2 sequences were available in GenBank, we initially amplified AGMMx2 from cDNA using primers complementary to the human Mx2 5′ and 3′ untranslated regions. PCR-amplified DNA was cloned, and 12 clones were sequenced. A single clone was subsequently used as a PCR template to amplify AGMMx2 for insertion into the lentiviral expression system. Species variants of Mx2 were amplified using the following primers: MacMx2, 5′-CTC TCT GGC CGA GAG GGC CAT GTC TAA GGC CCA CAA GTC TTG GC-3′ and 5′-TCT CTC GGC CAG AGA GGC CTC AAT GGA TCT CTT TGC TGG AGA ATT G-3′; AGMMx2, 5′-CTC TCT GGC CGA GAG GGC CAT GTC TAA GGC CCA CAA GTC TTG GC-3′ and 5′-TCT CTC GGC CAG AGA GGC CTT CAA TGG ATC TCT TCG CTG GAG AAT TG-3′; OvMx2, 5′-CTC TCT GGC CGA GAG GGC CAT GTC GAT GTC CTA TAG GGC TTT GAA G-3′ and 5′-TCT CTC GGC CAG AGA GGC CTC ATA TGC TTT TGA AAT GGG GGA ATT C-3′; and CanMx2, 5′-CTC TCT GGC CGA GAG GGC CAT GTC TAA GGC CCA CGG TTC TC-3′ and 5′-TCT CTC GGC CAG AGA GGC CTT AAC TGA AGA ACA TGT AGA GTG CGC-3′.

Chimeric Mx2s were generated using overlapping PCR with the primers listed above and also the following primers: $Can_{58}Hs$, 5′-AGG TGG GAG TGC AGG ATC CGG TTT ATC TCG CCA AGG ACT TCA ACT TTC TCA CTT TGA AC-3′ and 5′-CTG ATT GTT CAA AGT GAG AAA GTT GAA GTC CTT GGC GAG ATA AAC CGG ATC CTG CAC TC-3′; $Hs_{58}Can$, 5′-GCA GAG AAG GAC GCT GCT TTC CTC GCC AAG GAG TTC AAT TTG CTG ACA CTG AAC C-3′ and 5′-CTG GGG GTT CAG TGT CAG CAA ATT GAA CTC CTT GGC GAG GAA AGC AGC GTC CTT CTC TG-3′; $Can_{29}Hs$, 5′-AGA AAA AGA AAT GAA TTT TGT CCA GCA GCA GCC GCC GCC ATT CGG CAC AGT GCC ACC AC-3′ and 5′-GAA ACA TCA TTT GTG GTG GCA CTG TGC CGA ATG GCG GCG GCT GCT GCT GGA CAA AAT TC-3′; $Hs_{29}Can$, 5′-GAA AAA AGA AAT GAA TTC CTT CCA GCA ACA GCC ACC GCC ATC TGA CGC GGC AGC AAG GC-3′ and 5′-CTT GCT GCC GCG TCA GAT GGC GGT GGC TGT TGC TGG AAG GAA TTC ATT TCT TTT TTC AG-3′; $Mac_{90}AGM$, 5′-CAG GAA ACA CGA GCC AGC CAA GGG CAA AGG GGC CCG AGA ACA ACC TGC ACA GCC AGT AC-3′ and the SfiI-ApaI fragment of MacMx2; $AGM_{90}Mac$, 5′-AGG AAA CAC GAG CCA ACC AAG GGC AAA GGG GCC CGA GAA CAA CCT GCA CAA CCA GTA CG-3′ and the SfiI-ApaI of AGMMx2; $Mac_{333}AGM$, 5′-GGG GCA CCG AGA AAA GCA TCA TTA ATG TGG TAC GGA ACC TCA CAT ACC CCC TCA AGA AG-3′ and 5′-TGT AGC CCT TCT TGA GGG GGT ATG TGA GGT TCC GTA CCA CAT TAA TGA TGC TTT TCT CG-3′; $AGM_{333}MAC$, 5′-GAA CCT CAC ATA CCC CCT CAA GAA GGG CTA CAT GAT CGT GAA GTG CCG GGG CCA GCA GG-3′ and 5′-GAT GAT CTC CTG CTG GCC CCG GCA CTT CAC GAT CAT GTA GCC CTT CTT GAG GGG GTA TG-3′; HsRTA, 5′-CCT TCC AGC AAC AGC CAC CGC CAT TCC GCA CAG CGC CAC CAC AAA TGA TGT TTC CTC C-3′ and 5′-GGA GGA AAC ATC ATT TGT GGT GGC GCT GTG CGG AAT GGC GGT GGC TGT TGC TGG AAG G-3′; AGMGTV, 5′-TCC AGC AAC AGC CAC CGC CAT TCG GCA CAG TGC CAC CAC AAA TGA TGT TTC CCC CAA AC-3′ and 5′-TTG GGG GAA ACA TCA TTT GTG GTG GCA CTG TGC CGA ATG GCG GTG GCT GTT GCT GGA AG-3′; MacG37R, 5′-CTT CCA GCA ACA GCC ACC GCC ATT CCG CAC AGT GCC ACC ACA AAT GAC GTT TCC C-3′ and 5′-GGG AAA CGT CAT TTG TGG TGG CAC TGT GCG GAA TGG CGG TGG CTG TTG CTG GAA G-3′; and AGMR37G, 5′-CTT CCA GCA ACA GCC ACC GCC ATT CGG CAC AGC GCC ACC ACA AAT GAT GTT TCC C-3′ and 5′-GGG AAA CAT CAT TTG TGG TGG CGC TGT GCC GAA TGG CGG TGG CTG TTG CTG GAA G-3′.

The tetracycline-inducible lentiviral expression vector (pLKO.dCMV.TetO/R) used in the present study was constructed by the transfer of a unique 2,150-bp SpeI/BamHI fragment (containing sequences related to the hPGK promoter, the Tet repressor, and internal ribosome entry site [IRES]) from pLKO.Tet-ON (21) into pLKO.dCMV.TetO (22) (replacing complementary promoter sequences upstream of the puromycin resistance gene). The unique SfiI site in this vector was destroyed using the following oligonucleotides 5′-CTC GAG ACT AGT GCC T-3′ and 5′-CAC TAG TCT CGA GAG G-3′. Myc-tagged HsMx2 was then PCR amplified (from pLHCX-myc-HsMx2) using the following primers 5′-CTC TCT GCT AGC ACC ATG GAG CAG AAA CTC ATC TCT GAA G-3′ and 5′-CTC TCT GTC GAC GGC CAG AGA GGC CTC AGT GGA TCT-3′ before being subcloned into the LKO-derived vector above using NheI and SalI sites (leaving the following sequence, located between the forward primer and the start codon of Mx2: AGG ATC TGG CCG AGA GGG CC). This generated the vector pLKOΔ-MycHsMx2-IP and subsequent open reading frames (ORFs) of interest were inserted directionally into this vector, using SfiI (retaining the N-terminal tag). These ORFs are situated downstream of a truncated human cytomegalovirus immediate early promoter containing a tandem TetO operator sequence (22), allowing for the inducible expression of proteins in the presence of doxycycline. The pLKOΔ-HA-Mx2-IP vectors were generated by digesting pLKOΔ-MycTagRFP-IP with NheI and EcoRV, and the HA-SfiI-HpaI-SalI-SfiI multiple cloning site was generated by using the oligonucleotides 5′-CTA GCC ACC ATG TAC CCA TAC GAT GTT CCA GAT TAC GCT AAG GCC GAG AGG GCC GTT AAC GTC GAC GGC CTC TCT GGC CGT CGA-3′ and 5′-TCG ACG GCC AGA GAG GCC GTC GAC GTT AAC GGC CCT CTC GGC CTT AGC GTA ATC TGG AAC ATC GTA TGG GTA CAT GGT GG-3′.

Cell lines. Human T cell lines were maintained in RPMI. Human HEK293T, macaque FrHK4, canine MDCK, and AGM Vero cells were all maintained in Dulbecco modified Eagle medium (DMEM). Ovine CPT-Tert cells are choroid plexus cells immortalized with the simian virus 40 T antigen and human telomerase reverse transcriptase and were kindly pro-

vided by David Griffiths (23). CPT-Tert cells were grown in Iscove modified Dulbecco's medium (IMDM). IMDM, DMEM, and RPMI medium was supplemented with 9% fetal calf serum. Variants of Mx2, *Macaca mulatta* TRIM5 (Mamu1 EF113914), *Macaca mulatta* TRIMCyp (EU157763), and TagRFP doxycycline-inducible cell lines were generated through transduction with modified LKO-derived lentiviral vectors, followed by selection in either 2 μg of puromycin (Sigma)/ml or 1 mg of G418 (Invitrogen)/ml. G418-resistant vectors were used in MT-4 TMZ R5 cells, and puromycin-resistant vectors were used in all other experiments. Expression was induced in these cell lines through an overnight treatment with 125 ng of doxycycline hyclate (Sigma)/ml prior to challenge with retroviruses or retroviral vectors. MT-4 TMZ R5 cells are derived from MT-4 cells. They stably express CCR5 and encode an LTR-GFP reporter construct (T. M. Zang and P. D. Bieniasz, unpublished data).

Viruses, viral vectors, and infectivity assays. For replication-competent proviral clones we used pNHG (JQ585717), pNHGcapNM (JQ686832), pNL4-3 (M19921), and pCMO2.5 (24). All of the retroviruses and retroviral vectors used in the present study were generated through transfection of HEK293Ts using polyethyleneimine and titrated as described previously (25, 26). Briefly, viral stocks were titrated onto cells, and infected cells were quantified using flow cytometry. Titers were derived from at least three measurements at multiplicities of infection between 0.01 and 0.4. Cyclosporine (Sandoz) and Debio-025 (Novartis) were diluted in dimethyl sulfoxide and added to cultures at the time of infection, where indicated, at 5 μM.

For the CA mutant screen, purified plasmid DNA containing the green fluorescent protein (GFP)-encoding provirus NHGcapNM (accession JQ686832) and I2L, N5D, I6T, M10I, M10L, Q13H, A14S, I15V, N21S, S33C, Q50H, N57S, M68L, L69I, E75D, V83M, H87Q, H87R, P90T, I91T, I91V, Q95L, M96I, M96T, E98D, R100S, N121I, R132G, S146C, T148I, S149C, S149G, I150V, L151I, I153T, Y164F, R167Q, A177S, M185I, E187V, L190M, T200S, A204G, G208E, A209V, L211I, and T216A mutants thereof, were used to transfect HEK293T cells as described previously (27). Importantly, although some of these mutants have been classified as nonviable in spreading/replication assays (using <2% of the wild-type threshold [27]), all of the mutants were selected since they produce measurable titers of infectious virus in single-cycle transient-transfection/infection assays (the method used for the Mx2 screen). Filtered supernatants were titrated on doxycycline-treated MT-4 cells encoding HsMx2, MacMx2, AGMMx2, OvMx2, or CanMx2 in addition to untreated cells. Infected cultures were treated with dextran sulfate to limit infection to a single cycle (16 h postinfection) as described previously (27). All cells were fixed at 48 h postinfection and subjected to flow cytometry, and an infectious titer was calculated by counting GFP^+ cells.

For the HIV-1 adaptation and replication assays, doxycycline-treated or untreated MT-4 cells (modified to express doxycycline-inducible HsMx2) were infected with HIV-1 (pNHG, JQ585717), and infection was monitored every 24 h by flow cytometry as described previously (10, 28). Filtered (0.45-μm pore size) culture supernatants were used to inoculate fresh MT-4 cells when the majority of the cells became infected. At 28 days after the initiation of infection, DNA was extracted from infected cells using a "rapid isolation of mammalian DNA" protocol (DNA from cells infected with the parental clone was used as a control) (29). DNA encoding CA was PCR amplified using the following primers 5′-CAA CCA TCC CTT CAG ACA GGA TCA G-3′ and 5′-TTT TGG CTA TGT GCC CTT CTT TGC C-3′, and the amplicon was sequenced directly (Beckman Coulter Genomics). The same DNA extracted from infected cells was used as a template to amplify CA DNA for insertion into pNHGcapNM, as described previously (27). Multiple clones were sequenced in this context prior to characterization of the predominant P207S, G208R, and T210K CA mutants.

Western blot analyses. Cell lysates, were resolved using 4 to 12% acrylamide gels, blotted onto nitrocellulose membranes, and probed with anti-c-Myc (9E10 hybridoma) or anti-actin (JLA20 hybridoma) antibodies (both provided by the Developmental Studies Hybridoma Bank at the University of Iowa). Membranes were then probed with fluorescently labeled goat anti-mouse secondary antibodies (Thermo Scientific) prior to scanning with a Li-Cor Odyssey scanner.

Microscopy. Mx2 cDNAs from the various species were inserted into the HIV-1-based expression vector, HA-CSIB (18), which expresses N-terminally hemagglutinin (HA)-tagged proteins, followed by an IRES sequence and a blasticidin resistance cassette. In addition, chimeric Mx2s ($Hs_{29}Can$ and $Can_{29}Hs$) were inserted into pLKOΔ-HA-Mx2-IP, an HA-tagged derivative of pLKOΔ-MycHsMx2-IP. HOS cells were transduced with the HA-Mx2 expressing vectors, selected in antibiotic, and used as a pool for microscopy. Cells were seeded onto 24-well gelatin coated glass-bottom dishes (MatTek) and stained using anti-HA (Covance) and anti-Nup98 (Cell Signaling Technology) antibodies, followed by goat anti-mouse Alexa 488-conjugated and goat anti-rabbit Alexa 594-conjugated secondary antibodies (Molecular Probes). Cells were visualized by deconvolution microscopy as described previously (30). Image generation and colocalization analysis were completed with the SoftWorx software suite (Applied Precision). Pearson coefficient values were derived for Mx2 and Nup98 colocalization by analysis of optical sections coincident with the dorsal nuclear surface for 5 to 16 individual cells.

Structural analysis. Analysis of CA mutants in the context of the HIV-1 capsid hexamer was done using MacPyMOL with PDB reference 3GV2 (31).

Phylogenetic analysis. Orthologous Mx2 sequences were downloaded from complete genomes in Ensembl 73 (September 2013) and concatenated with the sequences obtained through direct sequencing. The protein sequences were aligned using Clustal Omega (32) and converted to a codon alignment using PAL2NAL (33). The best substitution model to use for phylogenetic reconstruction was determined using the Bayesian information criterion in jModeltest (34). The maximum-likelihood tree was calculated in PhyML with 1,000 bootstrap replicates (35). The codon alignment was used to detect positive selection in the primate lineage using the following Mx2 sequences: *Homo sapiens* (NM_002463.1), *Pan troglodytes* (XM_001171751.3), *Pan paniscus* (XM_003823906.1), *Gorilla gorilla* (XM_004062835.1), *Pongo abelii* (XM_002830701.1), *Papio anubis* (XM_003895463.1), *Macaca mulatta* (NM_001079696.1), *Chlorocebus aethiops* (KJ650325), *Saimiri boliviensis* (KJ650326), *Aotus trivirgatus* (KJ650327), and *Macaca nemestrina* (pigtail) 1 (KJ650328) and 2 (KJ650329). Positive selection was estimated using the random effect likelihood (REL) method using Hyphy made available through the Datamonkey webserver (36) and using CODEML in PAML (37). For CODEML, the codon alignment was used to construct a maximum-likelihood phylogenetic tree using RaxML v7.2.8 (38). The resulting tree was midpoint rooted and was consistent with the known phylogenetic relationships of primates. The F3x4 model for codon frequencies was used for each model, and each nested pair of models was compared using a likelihood ratio test and evaluated using the chi-squared critical value: M0 versus M3, M1a versus M2a, and M7 versus M8.

RESULTS

Several, but not all, Mx2 orthologs exhibit anti-HIV activity. Orthologous antiviral factors frequently exhibit species-dependent activity that reflects the presence or absence of a host-pathogen molecular interaction. This interaction can occur at the interface of restriction (such as TRIM5α binding to retroviral capsids [39–42]) or antagonism (such as SIV Nef interacting with tetherin [43–46]). Accordingly, documenting species-dependent activity of restriction factors can identify sites in viral and cellular molecules that are critical for antiviral activity/antagonism.

Mx proteins are a family of genome encoded antiviral defenses whose activity has been confirmed in divergent vertebrates, including mammals (15), birds (47), and fish (48). Most mammalian Mx proteins are formed from two distinct lineages (Mx1/MxA or Mx2/MxB) that arose from an ancient duplication event.

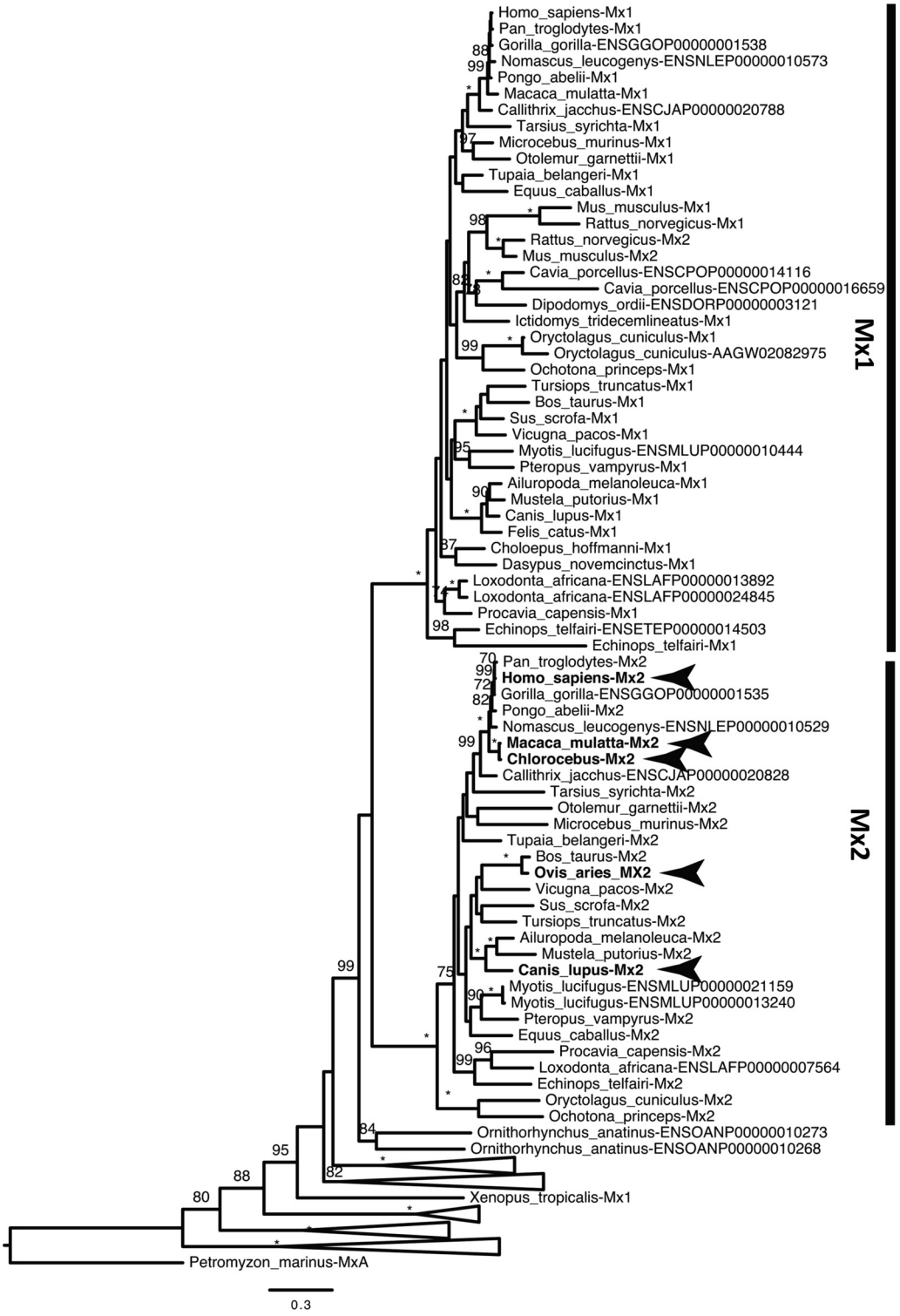

FIG 1 The Mx2 variants under investigation are orthologous. Maximum-likelihood phylogeny was calculated using the TIM2+I+G substitution model (log likelihood = −84,923.10). Bootstrap values below 70% are not shown for clarity, and asterisks (*) indicate 100% bootstrap support. The arrows indicate sequences functionally characterized in the present study.

Importantly, human Mx2 and murine Mx2 are not orthologous since murine Mx1 and Mx2 are paralogous members of the Mx1 lineage with the genuine ortholog of human Mx2 having been lost in rodent and felid lineages (Fig. 1). To investigate species-dependent variation in Mx2 antiretroviral activity, we expressed human (Hs), macaque (Mac), African green monkey (AGM), ovine (Ov), and canine (Can) species variants of Mx2 in a human $CD4^+$ T cell line (MT-4). Importantly, ovine and canine Mx2 are genuine or-

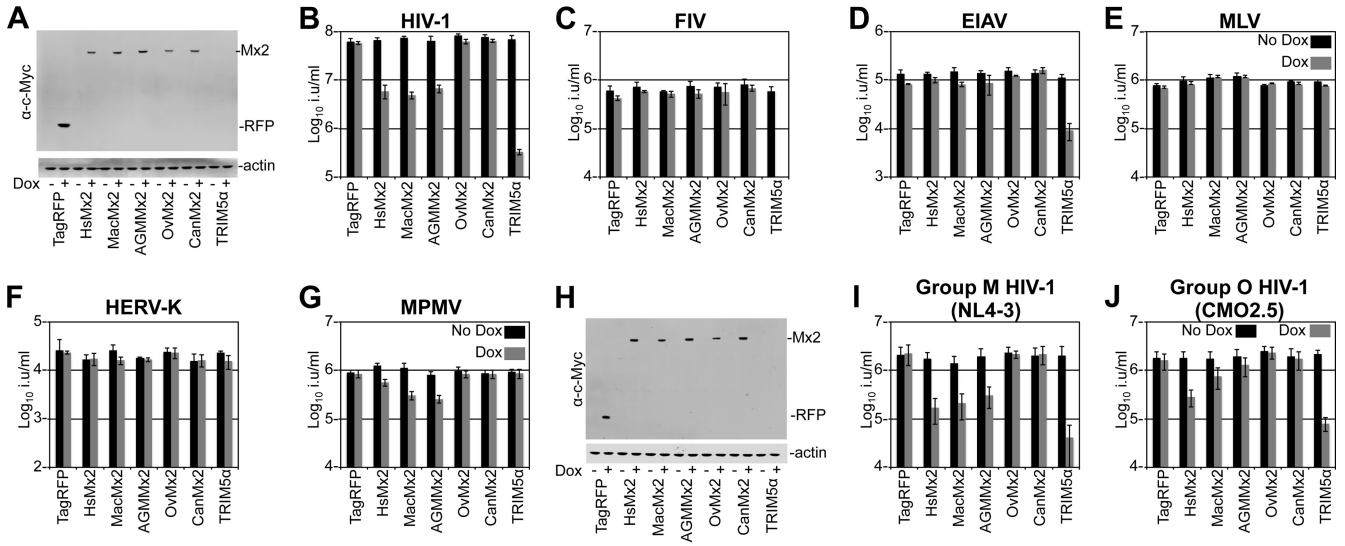

FIG 2 Multiple primate Mx2s inhibit HIV-1 infection, and group O is inhibited in a species-specific fashion. (A) Western blot analysis (α-c-Myc and α-actin) of HsMx2, MacMx2, AGMMx2, OvMx2, and CanMx2 (in addition to TagRFP and *Macaca mulatta* TRIM5α controls) expression in the MT-4 cells used throughout the manuscript (with the exception of Fig. 3 and 6), in the presence or absence of pretreatment with doxycycline. The level of infection of these MT-4 $CD4^+$ T cells expressing doxycycline-inducible variants of Mx2 (or TagRFP and *Macaca mulatta* TRIM5α controls) with (B) HIV-1 (pCCGW) (81), (C) FIV (pGiNSin) (82), (D) EIAV (pONY system), (E) MLV (pCNCG), (F) HERV-K (pCCGBX) (51), or (G) MPMV (pSARM-EGFP) (49) in the presence (gray bars) or absence (black bars) of pretreatment with doxycycline is shown. (H) Western blot analysis (α-c-Myc and α-actin) of HsMx2, MacMx2, AGMMx2, OvMx2, and CanMx2 expression (in addition to TagRFP and *Macaca mulatta* TRIM5α controls) in MT-4 TMZ R5 cells in the presence or absence of pretreatment with doxycycline. (I and J) Infection of MT-4 TMZ R5-expressing doxycycline-inducible variants of Mx2 (or TagRFP and *Macaca mulatta* TRIM5α controls) with (I) group M HIV-1 (NL4-3) and (J) group O HIV-1 (CMO2.5) in the presence (gray bars) or absence (black bars) of pretreatment with doxycycline.

tholog of human Mx2, based on our reconstructed phylogeny of Mx genes, confirming that all of the Mx2 proteins under investigation were part of the distinct Mx2 clade (Fig. 1). We next mimicked the natural interferon induction of Mx2 expression by using a tetracycline-inducible lentiviral expression system to introduce the Mx2 variants to these cells. Doxycycline-inducible TagRFP and rhesus TRIM5α (allele *Mamu1*) were included as negative and positive controls, respectively, in these and subsequent experiments. To allow direct comparison of the expression levels of divergent Mx2 orthologs, all of the variants were epitope tagged. After doxycycline induction, all of the species variants of Mx2 were expressed at similar levels, as determined by Western blotting (Fig. 2A). Strikingly, Mx2 from humans, macaques and African green monkeys all inhibited HIV-1 infection by ~10-fold, whereas ovine and canine Mx2s displayed no anti-HIV activity (Fig. 2B). Although TRIM5α was not readily visualized using Western blotting, it potently inhibited HIV-1 infection in this context (Fig. 2B, C, D, I, and J).

To further examine the spectrum of retroviruses inhibited by Mx2, we challenged our modified $CD4^+$ T cells with VSVG-pseudotyped GFP-encoding retroviruses that have previously been reported to be insensitive or less sensitive to human Mx2 (feline immunodeficiency virus [FIV], equine infectious anemia virus [EIAV], and murine leukemia virus [MLV] [18, 19]). In addition, because betaretroviruses circulated in human populations in our evolutionary past, we also examined whether MPMV (49, 50) and human endogenous retrovirus K (HERV K) (51) were sensitive to Mx2. FIV (Fig. 2C), EIAV (Fig. 2D), MLV (Fig. 2E), and HERV-K (Fig. 2F) were all insensitive to inhibition by all of the Mx2 variants tested. Surprisingly, MPMV (Fig. 2G) appeared to be partially sensitive to both MacMx2 and AGMMx2 (3- to 4-fold) and was minimally sensitive to HsMx2, suggesting that Mx2 antiretroviral activity might not be limited to primate lentiviruses and that Mx2 may be capable of inhibiting retroviruses from other genera.

HIV-1 group O is sensitive to human Mx2 but not AGM Mx2. Human Mx2 has been shown to be active against a variety of HIV-1 strains. However, all strains tested thus far are from the M group of pandemic HIV-1 strains. We tested the HIV-1 group O molecular clone CMO2.5 (24) and found it to be as sensitive as the group M clone NL4-3 to HsMx2 (Fig. 2I and J). In contrast, AGMMx2 potently inhibited infection of the group M virus (Fig. 2I) but was nearly inactive against the group O HIV-1 strain (Fig. 2J). MacMx2, which is nearly identical to AGMMx2, was partially active against the group O HIV-1 strain. These data clearly demonstrate that an extant retrovirus, specifically HIV-1 group O, can exhibit differential sensitivity to active Mx2 proteins from different species. Thus, similar to other antiviral factors, species variants of Mx2 can possess divergent antiviral specificities and inhibit different spectra of viruses.

Species variants of Mx2 can vary in their subcellular localization. To investigate why the Mx2 proteins varied in their ability to inhibit retroviral infection, we first examined their subcellular localization. Deconvolution microscopic analysis revealed that MacMx2 and AGMMx2 proteins were associated with nuclei and were particularly concentrated at nuclear pores, marked by the nucleoporin Nup98 (Fig. 3A and B). In this respect, the MacMx2 and AGMMx2 proteins were indistinguishable from HsMx2. Importantly, however, the nonprimate Mx2 proteins under investigation exhibited a different pattern of localization. In the case of ovine Mx2, the protein was almost entirely cytoplasmic, and little or no ovine Mx2 protein was found in association with nuclear pores (Fig. 3A, B, and C). For canine Mx2, two distinct patterns of

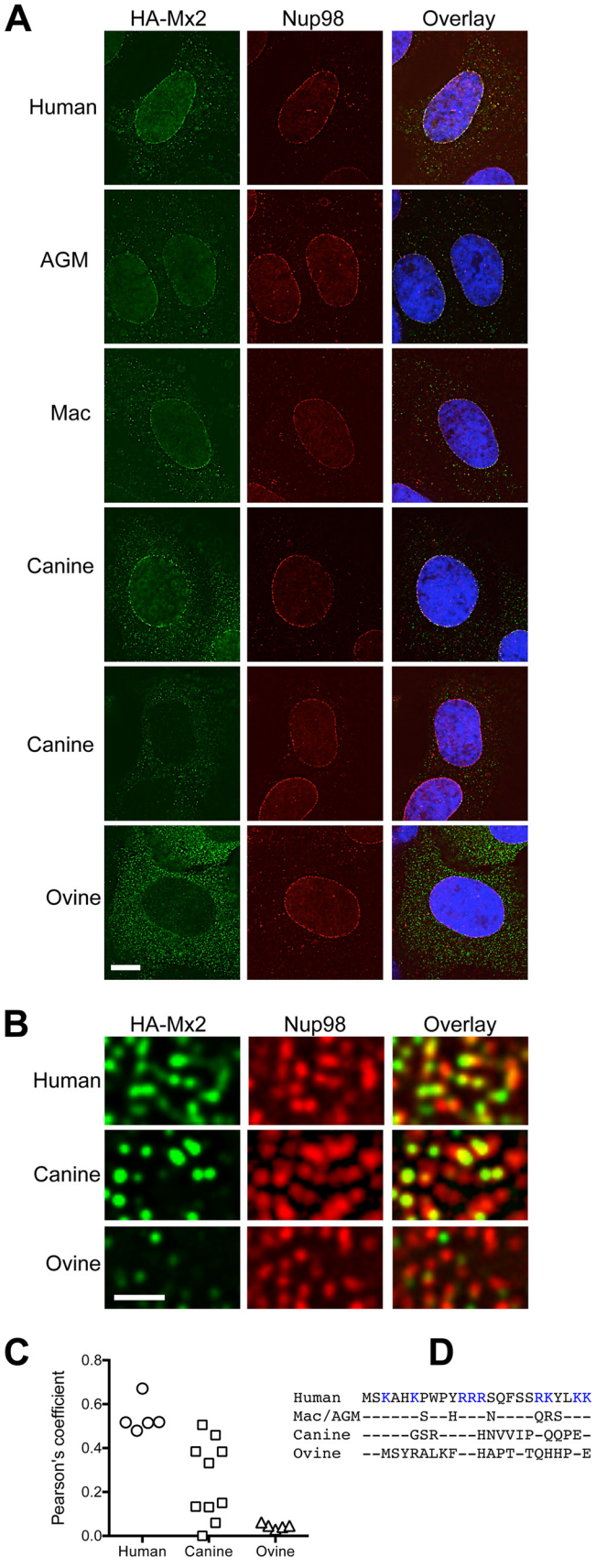

localization were observed. In ~60% of cells, which appeared to express higher levels of the protein, the distribution of canine Mx2 was similar to that of primate Mx2, i.e., there was a significant degree of colocalization with nuclear pores. However, in ca. 40% of cells, which appeared to express lower levels of the protein, there was little colocalization with Nup98 (Fig. 3A, B, and C).

Inspection of the N-terminal 25 amino acids of these Mx2 proteins revealed that the canine and especially the ovine Mx2 proteins were quite different in sequence from the primate Mx2 proteins (Fig. 3D). Notably, this segment of the human Mx2 protein has been demonstrated to be required for nuclear localization (16, 52) and contains a high density of basic amino acids, a frequent characteristic of nuclear localization sequences. Moreover, we have recently shown that these N-terminal amino acids are required for the anti-HIV-1 activity of HsMx2 (18). In canine and particularly ovine Mx2 proteins, several of the basic amino acids within the N-terminal segment are divergent, perhaps explaining the reduced propensity of these proteins to associate with nuclear pores and perhaps also their lack of antiretroviral activity.

The dependence of Mx2 antiviral activity on cyclophilin A is cell type dependent. We next considered the cyclophilin dependency of Mx2 antiviral activity. Previous observations suggest that the antiviral activity of Mx2 is dependent upon an interaction between the HIV-1 capsid (CA) and a host cyclophilin (20). Notably, while Mx2 expression protected $CD4^+$ SupT1 cells from HIV-1 infection, this antiviral activity was abrogated by the immunosuppressive drug cyclosporine (CsA) (20), which can disrupt cyclophilin-CA interactions. Accordingly, repeated passage of HIV-1 in the same Mx2-expressing cells selected for HIV-1 variants bearing a substitution (A88T) within the cyclophilin binding loop of CA (20). In contrast to these observations, in $CD4^+$ MT-4 cells, Mx2 inhibition of HIV-1 infection remained intact in the presence of either CsA or the synthetic CsA analogue Debio-025 (D025) (53) (Fig. 4A). Under identical conditions, both CsA and D025 completely recovered lentiviral infection (SIVagmTAN) in the presence of a macaque TRIMCyp allele (25, 26, 54), confirming that both drugs were biologically active under these conditions (Fig. 4A). These data indicate that an interaction between CA and cyclophilin is not necessary for Mx2 antiviral activity in all cell types.

Multiple determinants in HIV-1 CA govern sensitivity to Mx2. The observation that CsA did not rescue HIV-1 infection in the presence of Mx2 in MT-4 cells, led us to investigate whether HIV-1 could escape Mx2 via mutations at sites outside the cyclo-

FIG 3 Variation in subcellular localization among Mx2 proteins. (A and B) Deconvolution microscopic images of HOS cells stably expressing HA-tagged Mx2 proteins from the indicated species and stained with antibodies against the HA tag (green) and Nup98 (red). An overlay image, also displaying DAPI-stained nuclei, is also shown. In panel A, optical sections approximately at the center of the vertical dimension of the nucleus are shown, and the scale bar represents 5 μm. Two examples of cells expressing canine Mx2 are shown to reflect the diversity in localization that was observed for this particular Mx2 protein. In panel B, an expanded segment of an optical section coincident with the dorsal surface of the nucleus is shown, and the scale bar represents 1 μm. (C) Pearson correlation coefficient for colocalization of Nup98 and HA-Mx2 proteins from the indicated species. Each symbol represents the Pearson correlation coefficient for an individual cell. (D) Alignment of the N-terminal 25 amino acids of Mx2 from primates and nonprimates. Arginine and lysine residues (predicted to be important for nuclear localization) are highlighted in blue.

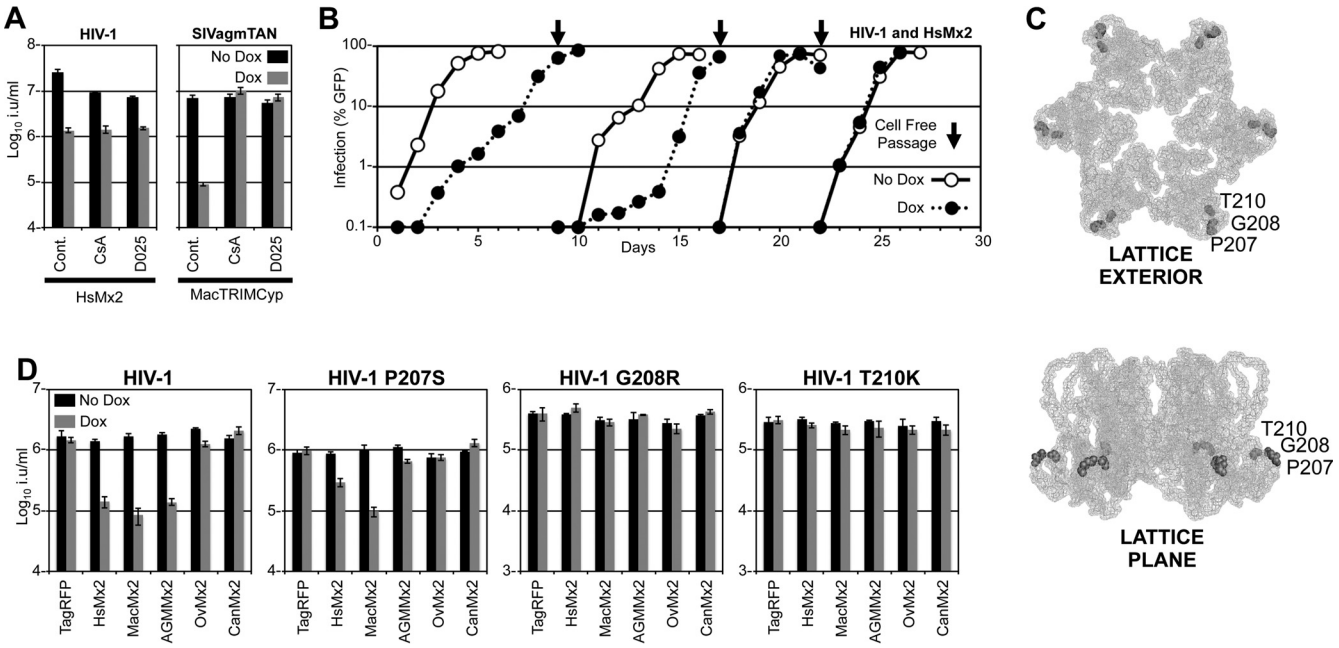

FIG 4 *In vitro* evolution reveals an Mx2 sensitivity determinant in the C-terminal domain of CA. (A) The level of infection with HIV-1 (NHG) or SIVagmTAN in cells expressing doxycycline-inducible HsMx2 or macaque TRIMcyp in the presence (gray bars) or absence (black bars) of pretreatment with doxycycline and the presence or absence of 5 μM CsA or D025 is shown. (B) The level of HIV-1 (NHG) infection in cells expressing doxycycline-inducible HsMx2 treated (filled circles, dashed line) or not treated (unfilled circles, solid line) with doxycycline is shown over time. Cell-free passages are indicated with arrows. (C) The positions of P207S, G208R, and T210K point mutants are highlighted as solid gray spheres on the CA hexamer structure (3GV2). (D) The level of infection of MT-4 $CD4^+$ T cells expressing doxycycline-inducible Mx2 variants (or TagRFP control) with HIV-1 (NHGcapNM) or P207S, G208R, or T210K point mutants in the presence (gray bars) or absence (black bars) of pretreatment with doxycycline is shown.

philin binding loop, if pressured to do so in cells where CsA does not rescue infectivity. To investigate this possibility, we passaged HIV-1 in the presence of HsMx2 for 4 weeks in $CD4^+$ MT-4 cells. To facilitate the quantitation of HIV-1 infection, we used a replication-competent proviral clone in which *nef* was replaced with enhanced green fluorescent protein (EGFP; NHG). During the first 2 weeks, replication kinetics were substantially delayed in Mx2 expressing MT-4 cells compared to noninduced controls (Fig. 4B). However, at the third passage, and at subsequent time points, the viral replication kinetics were similar, regardless of the presence of HsMx2 (Fig. 4B). We extracted DNA from the population of HsMx2-expressing infected cells at the end of the fourth passage, and the CA region of *gag* was PCR amplified and sequenced. Analysis of the resulting chromatogram indicated a "hot spot" of variation in the region encoding CA residues 207 to 210 (Fig. 4C). Sequencing of multiple clones indicated that the variation within the swarm was due to the presence of three separate lineages, each bearing a single CA mutation (P207S, G208R, or T210K), rather than the presence of double or triple mutants. Therefore, we generated three viral clones bearing the P207S, G208R, or T210K substitutions, in isolation. Although the parental clone was sensitive to all of the primate variants of Mx2 (Fig. 4D), the G208R and T210K variants were entirely insensitive to any of the Mx2 variants tested (Fig. 4D). Strikingly, the P207S variant behaved differently. Although this virus was partially resistant to human Mx2, this virus was fully sensitive to macaque Mx2 but entirely resistant to the nearly identical AGMMx2 (Fig. 4D). Importantly, these data indicate not only that single substitutions in CA can govern sensitivity to Mx2 activity but that divergent Mx2 variants can differentially inhibit viruses that differ by just a single CA residue. Thus, these data further suggest that, similar to other genome encoded antiviral defenses, species variants of Mx2 have divergent antiviral specificities.

The unanticipated identification of residues in the C-terminal domain of CA (Fig. 4C) that conferred resistance to Mx2-mediated antiviral activity led us to consider whether additional regions of CA might confer resistance to Mx2. We recently described a library of CA mutants that we used to probe the genetic robustness of this region of *gag* (27). In an attempt to identify more substitutions that might confer resistance to Mx2, we challenged $CD4^+$ MT-4 T cells expressing species variants of Mx2 with 46 CA mutants from this library that produced an easily measurable infectious titer in single cycle infection assays (Fig. 5A). In accordance with our previous observations, ovine and canine variants of Mx2 did not substantially inhibit any of the mutants in the library (Fig. 5A). In contrast, while primate Mx2s inhibited the majority of HIV-1 CA mutants, seven substitutions in CA conferred resistance to one or more primate variants of Mx2 (Fig. 5A). Five of these substitutions reduced the sensitivity to all of the primate variants tested (M10I, N57S, H87R, P90T, and Q95L). In addition, two substitutions, M185I and E187V, conferred resistance to HsMx2 and AGMMx2, respectively. In order to validate the library screen, the infectivity of independent preparations of these seven mutants was quantified in cells expressing each of the species variants of Mx2 (Fig. 5C).

In agreement with our own and others' previous findings, mutations in the cyclophilin binding loop conferred resistance to Mx2. Specifically, mutations at CA residues 88 to 90, 92, and 94 have all been shown to reduce the sensitivity of HIV-1 to human Mx2 (13, 18, 20). Our screen identified a P90T substitution (Fig. 5B and C) that

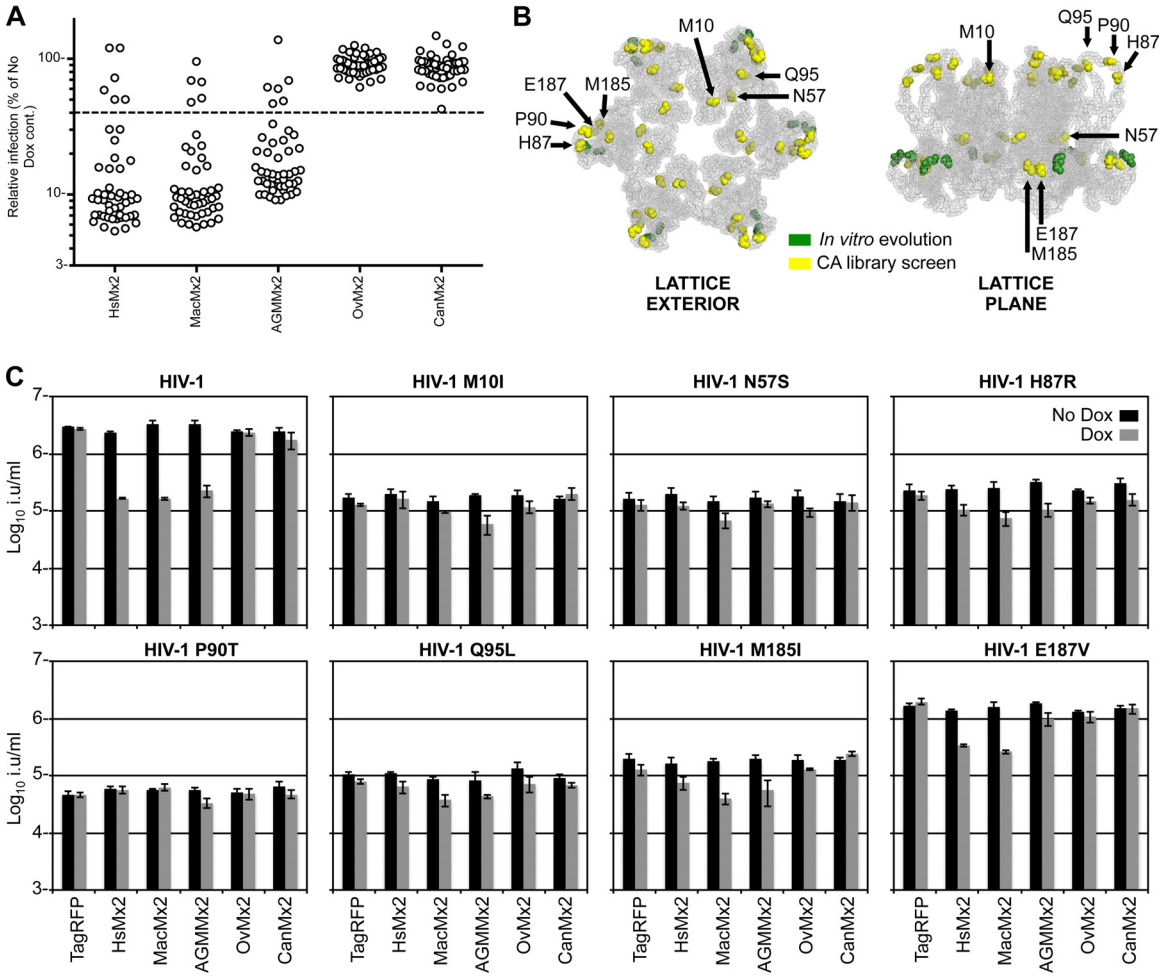

FIG 5 CA library screening identifies multiple substitutions conferring resistance to Mx2. (A) The level of infection (relative to non-doxycycline-treated controls) of 46 HIV-1 CA mutants in doxycycline-treated MT-4 $CD4^+$ T cells expressing doxycycline-inducible Mx2. The dashed line indicates the threshold used to select resistant mutants for further consideration. (B) The positions of the seven point mutants most resistant to Mx2 identified in panel A are highlighted as yellow spheres on the CA hexamer structure (3GV2). Residues identified through *in vitro* evolution are also highlighted as green spheres. (C) The level of infection of MT-4 $CD4^+$ T cells expressing doxycycline-inducible Mx2 variants (or TagRFP control) with HIV-1 (NHGcapNM) or the indicated CA point mutants in the presence (gray bars) or absence (black bars) of pretreatment with doxycycline is shown.

conferred complete resistance to all of the Mx2 variants tested. Moreover, the screen identified two additional mutants (H87R and Q95L), flanking those previously described that conferred substantial, but incomplete, resistance to Mx2. Notably, while these data highlight the importance of the cyclophilin binding loop as an Mx2 sensitivity determinant, the inability of CsA to rescue infectivity in the same cells suggests that the Mx2 resistance conferred by mutations in the cyclophilin binding loop is not solely due to the loss of an interaction with cyclophilin A (CypA).

The CA library screen also identified two other residues in the N-terminal domain of CA that promoted escape from Mx2 (Fig. 5B and C). We have previously described one of these residues (N57S) and suggested that the inability of this mutant to infect nondividing cells might underlie its reduced sensitivity to Mx2 (18, 55). Accordingly, this mutant conferred nearly complete resistance to each of the primate Mx2s. In addition, we identified a substitution in the β-hairpin close to the N terminus of CA (M10I) that also confers near complete resistance to Mx2 (Fig. 5B and C). Interestingly, like cyclophilin binding loop residues, this CA residue forms part of the cytosolic surface of the mature CA that is readily accessible to inhibitory interactions. Moreover, the same substitution, and cyclophilin binding loop residues, have previously been implicated in escape from TRIM5α (28, 56).

Outside of the CA N-terminal domain, the screen identified additional residues in the C-terminal domain of CA that influence sensitivity to Mx2 (M185I and E187V). Residue M185 is buried within intact cores and forms an important hydrophobic contact at the C-terminal domain of the CA dimerization interface (57). Although neither M185I nor E187V substitutions conferred complete resistance to all tested primate Mx2 proteins (Fig. 5C), in accordance with the initial CA library screen, M185I was substantially less sensitive to HsMx2 and the E187V mutant was almost completely resistant to AGMMx2. Interestingly, E187 is in close proximity to P207 and G208, further highlighting the importance of this region as a C-terminal Mx2 sensitivity determinant (Fig. 5B). Notably, all of the CA substitutions that result in species-specific sensitivity to primate Mx2s occur within this localized region of the C-terminal domain. Although the CA C-terminal domain is

not usually implicated in mediating interactions with host factors, residues P207, G208, and T210 form the majority of a solvent accessible loop between helices 10 and 11. This sequence is exposed to the host cytosol in the context of the mature fullerene core, albeit at a position that is significantly recessed relative to the protruding CA N-terminal domains. Thus, it is possible that host factors could interact directly with this sensitivity determinant in the context of intact cores. Alternatively, it is also conceivable that these mutations exert their effect through changes in capsid morphology or stability (58) or through varying the pathway used to traverse the nuclear pore (55, 59–61). A confounding variable in these analyses is the fitness reduction observed for many of the substitutions conferring resistance to Mx2 (Fig. 4 and 5). An increase in noninfectious particles in the inoculum could, in principle, saturate Mx2 antiviral activity, leading to apparent resistance. Importantly, however, the P207S and E187V substitutions confer resistance while maintaining fitness levels similar to the parental clone. Moreover, several substitutions that also attenuate replicative fitness (L69I, N121I, R132G, and L211I [27]) did not confer resistance to Mx2.

An 8-amino-acid segment of the N terminus of Mx2 can determine antiviral specificity. The observation that some variants of Mx2 have no apparent antiretroviral activity, coupled with the species-dependent antiviral specificity of primate Mx2s, prompted us to assemble chimeric Mx2 molecules to identify the region(s) of Mx2 that determine antiviral activity and specificity. First, we made chimeras between human and canine Mx2s (Fig. 6A to C). Our initial human-canine chimeras suggested the importance of the N-terminal region of Mx2 (unpublished observations). This led us to make further chimeras focusing on this N-terminal region. Replacing the N-terminal 58 residues of canine Mx2 with the corresponding region of human Mx2 ($Hs_{58}Can$) generated a chimeric Mx2 that efficiently inhibited HIV-1 infection (Fig. 6B). In contrast, the reciprocal chimera had no anti-HIV-1 activity despite being expressed at similar levels (Fig. 6C), indicating that a major antiviral activity/specificity determinant lies within the N terminus of Mx2. To further map this determinant, we replaced the N-terminal 29 amino acids of CanMx2 with HsMx2 ($Hs_{29}Can$). As before, this chimeric Mx2 efficiently inhibited HIV-1 infection, whereas the reciprocal chimera had no anti-HIV-1 activity (Fig. 6B), despite similar levels of expression (Fig. 6C). The inhibitory action of these chimeras indicates that a major antiviral activity/specificity determinant resides within the first 29 amino acids of Mx2. Interestingly, the N-terminal region of Mx2 is the most divergent section of mammalian Mx2 proteins. Moreover, it contains the determinant that is required for nuclear localization, which is more robust in the case of the primate Mx2 proteins than for canine Mx2 (Fig. 3).

Because the N-terminal region of human Mx2 is required for correct nuclear localization (16, 52), we reasoned that replacing the first 29 residues of canine Mx2 with those of human Mx2 would generate a chimeric Mx2 whose localization was reminiscent of primate Mx2. Indeed, deconvolution microscopic analysis revealed that the $Hs_{29}Can$ chimera was associated with nuclei and was particularly concentrated at nuclear pores, marked by the nucleoporin Nup98 (Fig. 6D and E). In this respect, the chimeric protein was indistinguishable from HsMx2. In contrast, the reciprocal chimera exhibited a different pattern of localization. In the presence of the canine N terminus, two distinct patterns of localization were observed. Similar to canine Mx2, in ~60% of cells there was a significant degree of colocalization with nuclear pores. However, in ca. 40% of cells, there was little colocalization with Nup98 (Fig. 6D and E). The correlation between nuclear pore localization and anti-HIV-1 activity suggests that localization to the nuclear pore could be a requirement for anti-HIV-1 activity.

To further investigate Mx2 antiviral specificity and remove the variable of differential localization that might confound an analysis of CanMx2/HsMx2 chimeras, we made chimeras between the closely related (99% identical), nuclear-pore-localized, macaque and AGM Mx2 proteins (Fig. 6F to I). Of these two Mx2 proteins, only macaque Mx2 inhibits the P207S HIV-1 CA mutant (Fig. 4D). Therefore, we could exploit this observation to uncover which amino acids define the divergent specificities of these nearly identical factors. In accordance with the human-canine chimeras, replacing the N-terminal 333 amino acids of AGMMx2 with the corresponding region of MacMx2 generated a chimeric Mx2 ($Mac_{333}AGM$) that efficiently inhibited infection of the P207S CA mutant. In contrast, the reciprocal chimera had no activity against the P207S virus but retained activity against the parental HIV-1 clone (Fig. 6G). To further map this specificity determinant, we replaced the N-terminal 90 amino acids of AGMMx2 with the same region of MacMx2 ($Mac_{90}AGM$). Because MacMx2 and AGMMx2 are so closely related, this chimera differs at just three positions from AGMMx2 (Fig. 6I), and these three changes are concentrated in an 8-amino-acid stretch (residues 37 to 44). Remarkably, substituting these three residues ($Mac_{90}AGM$) completely transferred antiviral specificity and generated a chimeric Mx2 that efficiently inhibited infection by the HIV-1 P207S mutant (Fig. 6G). In contrast, the reciprocal chimera ($AGM_{90}MAC$) had no activity against this mutant but retained the ability to inhibit infection with the parental HIV-1 strain. The observation that all AGM and macaque chimeras were able to inhibit the parental HIV-1 clone indicates that these chimeras were all active antiviral factors capable of inhibiting HIV-1 infection. Thus, amino acids 37 to 44 must constitute an antiviral specificity determinant within these functional Mx2 proteins. As before, Mx2 antiviral activity was also highly specific, and no inhibition of MLV infection was observed in the presence of any chimeric Mx2s. Considered together, these data suggest that a major antiviral specificity determinant of Mx2 resides in a localized 8-amino-acid segment close to the N terminus of Mx2.

In light of the observation that this 8-amino-acid region can govern Mx2 antiviral specificity for the HIV-1 P207S CA mutant, we reasoned that these same residues could define antiviral specificity for group O HIV-1. To investigate this possibility, we examined the ability of human and AGM chimeric Mx2s to inhibit group O HIV-1. Human and AGM Mx2 only differ at positions 37 and 39 within this 8-amino-acid region (Fig. 6J) so we constructed human and AGM Mx2s that were chimeric only at these two positions. Similar to human and AGM Mx2 variants, both chimeras were active against group M HIV-1 (NL4-3). Strikingly, despite being active against group M HIV-1, human Mx2 with AGM residues 37 and 39 (HsRTA) was unable to inhibit group O HIV-1 (Fig. 6K). Conversely, humanizing residues 37 and 39 of AGM Mx2 (AGMGTV) conferred potent anti-group O activity to this previously inactive variant (Fig. 6K). Importantly, these data highlight that residues within this localized antiviral specificity determinant can govern activity against HIV-1 derived from extant viruses. Thus, this region likely governs specificity for circulating viruses and is not limited to determining activity against HIV-1 CA mutants.

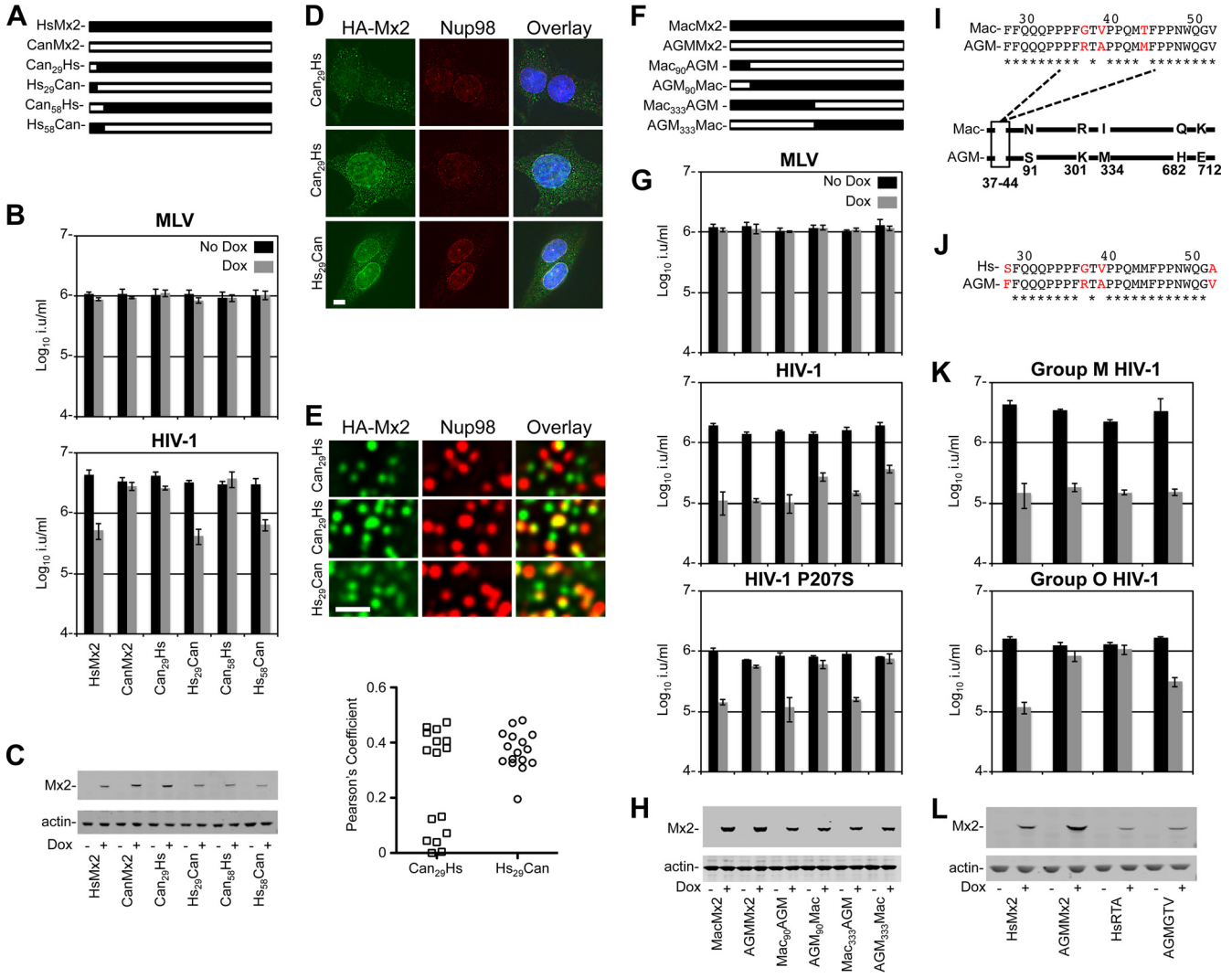

FIG 6 Chimeric Mx2s reveal an N-terminal antiviral specificity determinant. (A) Diagrammatic representation of the chimeric human and canine Mx2 proteins used in panels B and C. (B) The level of infection of MT-4 $CD4^+$ T cells expressing doxycycline-inducible HsMx2, CanMx2, or human-canine chimeric Mx2s with HIV-1 (NHG) or MLV (CNCG) in the presence (gray bars) or absence (black bars) of doxycycline pretreatment is shown. (C) Western blot analysis (α-c-Myc and α-actin) of HsMx2, CanMx2, and chimeric Mx2s in $CD4^+$ MT-4 cells in the presence or absence of doxycycline pretreatment (D) Deconvolution microscopic images of HOS cells stably expressing HA-tagged Mx2 proteins from the indicated chimera and stained with antibodies against the HA tag (green) and Nup98 (red). An overlay image, also displaying DAPI-stained nuclei, is also shown. In panel D, optical sections approximately at the center of the vertical dimension of the nucleus are shown, and the scale bar represents 5 μm. Two examples of cells expressing $Can_{29}Hs$ are shown to reflect the diversity in localization that was observed for this particular Mx2 chimera. In panel E, an expanded segment of an optical section coincident with the dorsal surface of the nucleus is shown, and the scale bar represents 1 μm. The Pearson correlation coefficient for the colocalization of Nup98 and HA-Mx2 proteins from the indicated chimera is also shown. Each symbol represents the Pearson correlation coefficient for an individual cell. (F) Diagrammatic representation of the chimeric macaque and AGM Mx2s used in panels G and H. (G) The level of infection of MT-4 $CD4^+$ T cells expressing doxycycline-inducible HsMx2, AGMMx2, or chimeric Mx2s with HIV-1 (NHGcapNM), HIV-1 P207S, or MLV (CNCG) in the presence (gray bars) or absence (black bars) of pretreatment with doxycycline is shown. (H) Western blot analysis (α-c-Myc and α-actin) of MacMx2, AGMMx2, and chimeric Mx2s in $CD4^+$ MT-4 cells in the presence or absence of pretreatment with doxycycline. (I) Diagrammatic representation of macaque and AGM Mx2 highlighting the regions of divergence between these orthologs. (J) Alignment of a short section of human (Hs) and AGM Mx2 highlighting divergent residues in this region. (K) The level of infection of MT-4 $CD4^+$ T cells expressing doxycycline-inducible HsMx2, AGMMx2, or chimeric Mx2s with group M HIV-1 (NL4-3) or group O (CMO2.5) HIV-1 in the presence (gray bars) or absence (black bars) of pretreatment with doxycycline is shown. (L) Western blot analysis (α-c-Myc and α-actin) of HsMx2, AGMMx2, and chimeric Mx2s in $CD4^+$ MT-4 cells in the presence or absence of pretreatment with doxycycline.

Signatures of positive selection are evident within the N-terminal specificity determinant of Mx2. The observation that primate Mx2s exhibit species-dependent antiviral activity raised the possibility that Mx2 and primate lentiviruses have been involved in a molecular "arms race" during primate evolution. Therefore, we investigated whether signatures of positive selection exist in primate Mx2 sequences. We confined this analysis to primate sequences since thus far we have only observed Mx2 antiviral activity against primate viruses. We subjected sequences from NCBI databases or generated as part of the present study to positive selection analysis. Using our data set, we calculated an average ratio of nonsynonymous to synonymous evolutionary changes

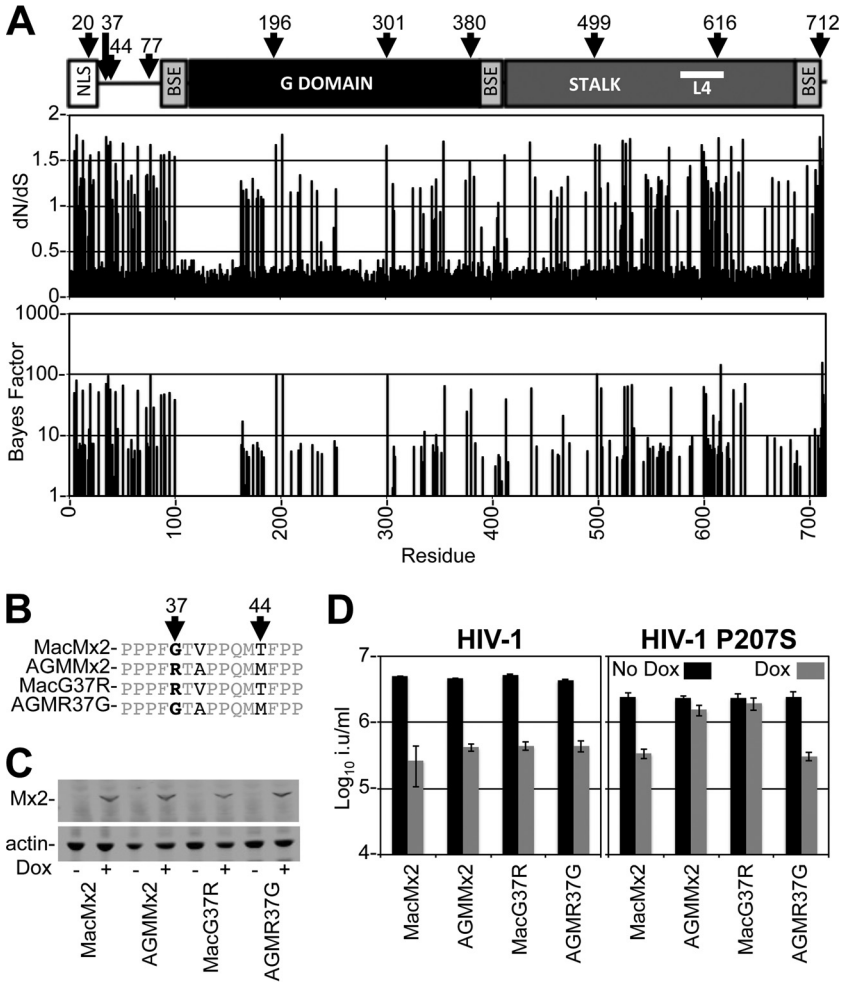

FIG 7 A single residue determines species-dependent inhibition of the HIV-1 P207S CA mutant. (A) A diagram representing the various domains of Mx2 is shown (BSE indicates the bundle signaling element), above plots of the *dN/dS* ratio (upper plot) and the Bayes factor for *dN>dS* (lower plot) at each codon in an alignment of primate Mx2 coding sequences. Ten residues identified by REL and M3 methods (from Table 1) are highlighted with arrows. The analogous loop 4 (L4) of Mx1 (62) is also highlighted. (B) Alignment of a short section of MacMx2 and AGMMx2 highlighting divergent residues in this region. (C) Western blot analysis (α-c-Myc and α-actin) of HsMx2, AGMMx2, and chimeric Mx2s in $CD4^+$ MT-4 cells in the presence or absence of pretreatment with doxycycline. (D) The level of infection of MT-4 $CD4^+$ T cells expressing doxycycline-inducible MacMx2, AGMMx2 or point mutants thereof with HIV-1 (NHGcapNM) or HIV-1 P207S in the presence (gray bars) or absence (black bars) of pretreatment with doxycycline is shown.

(*dN/dS*) of 0.44 using CODEML, a finding consistent with purifying selection having been the dominant selective force during Mx2 evolution. However, both the REL and CODEML methods identified codons with high *dN/dS* ratios (Fig. 7A). The nested models from CODEML were compared, and the M3 model gave a significantly better fit than the M0 model, suggesting that distinct selective pressures have acted on specific sites during primate evolution. The REL and M3 methods both identified a set of 10 positively selected sites with Bayes factors above 50 and posterior probabilities above 0.95 (listed in Table 1). Interestingly, two positively selected sites (residues 37 and 44) lie within the 8-amino-acid specificity determinant identified using chimeric macaque and AGM Mx2s. One of these sites, residue 37, had a *P* value of 0.998 and the highest Bayes factor within the N-terminal region (95.08), suggesting this residue could have been of particular importance during primate evolution. We therefore examined the ability of this residue to govern Mx2 antiviral specificity. Remarkably, making a single substitution at residue 37 was sufficient to alter Mx2 antiviral specificity. Specifically, replacing AGM Mx2 residue 37 with the corresponding macaque residue (AGMR37G) was sufficient to confer potent antiviral activity to AGMMx2 against the P207S HIV-1 CA mutant (Fig. 7D). Conversely, making the reciprocal substitution in macaque Mx2 (MacG37R) ablated antiviral activity against the P207S mutant (Fig. 7D). Crucially, both point mutants were expressed at similar levels (Fig. 7C) and were active against the parental HIV-1 clone (Fig. 7D). Thus, in this instance, amino acid 37 governs species-specific Mx2 antiviral activity against the HIV-1 P207S mutant.

DISCUSSION

Extant species are descended from ancestors that were each challenged by unique spectra of pathogens. Consequently, orthologous genome encoded antiviral defenses have been selected to inhibit divergent spectra of viruses. Here, we show that Mx2 exhibits species-dependent variation in antiviral specificity that is likely the result of diversity in ancient selective forces. All of the

TABLE 1 Positively selected sites consistent between CODEML model M3 and REL[a]

Codon	Residue (human)	M3 ω	M3 probability (ω > 1)	REL *dN/dS*	REL posterior probability	REL Bayes factor
20	K	1.826	1.000	1.562	0.960	70.23
37	G	1.641	0.998	1.668	0.970	95.08
44	M	1.880	1.000	1.469	0.947	52.09
77	R	1.640	0.998	1.677	0.971	99.74
196	V	1.629	0.998	1.676	0.972	101.27
301	R	1.616	0.998	1.668	0.970	95.50
380	M	1.614	0.998	1.500	0.951	57.17
499	K	1.618	0.998	1.681	0.972	102.44
616	N	1.689	0.999	1.752	0.980	145.53
712	K	1.712	0.999	1.764	0.982	157.75

[a] Model M3 was a significant improvement over M0 [2(dL) = 84.92, df = 4, $P < 0.01$]. Models M2a and M8 were not significant improvements over models M1a [2(dL) = 4.06, df = 2, NS] and M7 [2(dL) = 4.08, df = 2, NS], respectively. dL, log-likelihood difference; df, degrees of freedom; NS, not significant; ω, *dN/dS*.

primate Mx2 proteins tested were capable of inhibiting HIV-1, whereas canine and ovine orthologs had no such activity. Notably, transfer of a small region of human Mx2 to canine Mx2 conferred anti-HIV-1 activity, indicating that canine Mx2 requires little modification to gain this function. It is possible that antiretroviral activity of Mx2 proteins was gained specifically in the primate lineage or that antiretroviral activity arose earlier and ovine and canine Mx2 proteins inhibit retroviruses that have yet to be tested. Further work is required to support or exclude either possibility. Interestingly, the ovine Mx2 protein did not localize to nuclear pores, and canine Mx2 proteins did so less robustly than did the primate Mx2 proteins. Thus, it is possible that robust nuclear pore localization emerged in Mx2 proteins alongside the acquisition of activity against primate lentiviruses.

Species variants of Mx2s have divergent antiviral specificities. Notably O-group HIV-1, HIV-1 P207S, and to a lesser extent HIV-1 E187V were inhibited by primate Mx2 proteins in a species-dependent manner. Although HsMx2 inhibited all of these viruses, AGMMx2 did not (but was able to inhibit an M-group virus, namely, HIV-1 NL4-3). In at least one instance, a single residue (residue 37) close to the N terminus of Mx2 was responsible for this specificity. Moreover, residue 37 was one of two residues that also governed specificity for group O HIV-1. Sequence analysis revealed that, similar to other genome encoded antiviral factors, the majority of Mx2 residues are evolving under purifying selection (62, 63), which is likely driven by the requirement to maintain the structural and functional integrity of Mx2. Within this background, however, signatures of positive selection are apparent, particularly close to the N terminus of Mx2. Strikingly, residue 37, which we demonstrate to be one determinant of antiviral specificity, was identified as evolving under positive selection. This raises the possibility that the signatures of positive selection apparent near the N terminus of Mx2 could have been driven by antagonistic host-pathogen interactions. One such possible selective pressure could be the antilentiviral specifying activity of this region. We note, however, that it is unlikely that residue 37 is the only residue governing Mx2 antiviral specificity, since humanizing the first 29 residues of canine Mx2 also conferred anti-HIV-1 activity. In contrast, the reciprocal chimera, bearing the first 29 residues from canine Mx2 but retaining the original human residue at position 37, was rendered inactive against HIV-1. Thus, other determinants of antiretroviral activity or specificity exist within the first 29 residues of human Mx2. Further work is required to determine whether the first 29 residues solely specify a subcellular localization compatible with anti-HIV-1 activity or whether additional specificity/activity determinants reside within the extreme N-terminal region of Mx2.

Interestingly, the N-terminal region of Mx2, which determines antiviral specificity, is spatially distinct from the disordered loop 4 (L4) that has been uncovered as a major antiviral specificity determinant of the Mx1 protein (62). Mx1 has been proposed to directly bind viral components through the stalk domain (64, 65) and perhaps assemble into oligomeric arrays that stimulate GTPase activity and activate the antiviral function of the C-terminal effector domain (66). A predicted structure of Mx2 places the N-terminal specificity determinant proximal to the "hinge-like" bundle signaling element (67), spatially separated from L4. The distinct locations of these specificity determinants, considered alongside their differential dependence on GTPase activity (18, 19), reinforce the notion that the antiviral activity of the Mx2 protein is mechanistically distinct from that of Mx1.

In addition to inhibiting the infection of primate lentiviruses, Mx2 also inhibited the betaretrovirus MPMV, albeit relatively weakly. Although it is unlikely that such a modest inhibition would be relevant *in vivo*, this observation highlights the possibility that Mx2 could inhibit divergent retroviruses. It may be that other untested mammalian Mx2 proteins possess potent activity against betaretroviruses or other retroviruses. Such divergent activities could be important in understanding the evolutionary pressures that have shaped the activity of primate Mx2 proteins.

TRIM5α is a well-characterized antiviral factor that, like Mx2, blocks retroviral infection at an early stage postinfection. The surfaces of CA that are bound by *Macaca mulatta* TRIM5α have been extensively characterized for both MLV and HIV-1 (28, 40, 41, 56, 68, 69). When the CA surfaces defining TRIM5α and Mx2 sensitivity are compared, similarities are apparent. Substitutions in both the cyclophilin binding loop and the N-terminal β-hairpin reduced sensitivity to both antiviral factors (Fig. 5) (28, 56). Indeed, screens of the same HIV-1 CA library identified the same M10I and P90T substitutions, which confer escape from Mx2, as changes that reduce sensitivity to rhesus TRIM5α (28). Although multiple CA surfaces are important determinants of Mx2 sensitivity, not every change in these regions confers escape. For example, M10I and H87R substitutions desensitize HIV-1 to Mx2, whereas other changes at the same positions (M10L and the common polymorphism H87Q) do not. Clearly, both the position and the nature of the substitution in HIV-1 CA influence Mx2-sensitivity. Thus, the substitutions identified herein likely represent an un-

derestimate of the total number and extent of changes that could confer reduced sensitivity to Mx2. Moreover, a comparison of M-group (NL4-3) and O-group (CMO2.5) CA sequences suggests that none of the substitutions described here account for the differential susceptibility of these viruses to AGMMx2. Again, this suggests that more, perhaps many more, positions in CA that are yet to be described govern sensitivity to Mx2.

Despite the similarities, there are also substantial differences between the sensitivity determinants for Mx2 and TRIM5α. In particular, two additional CA surfaces appear to be important for Mx2 sensitivity. First, one important CA surface thought to mediate interactions with the host is the cleavage- and polyadenylation-specific factor 6 (CPSF6) binding interface (70, 71). Two substitutions in this region have been reported to facilitate escape from Mx2 (N74D [19] and N57S [18]). Although clearly important for Mx2 sensitivity, this binding interface is not generally considered important for interaction with TRIM5α. Second, although multiple CA residues influence sensitivity to TRIM5α, they overwhelmingly occur on the surface of the N-terminal domain of CA and, crucially, no major sensitivity determinants have been described in the C-terminal domain. Strikingly, both *in vitro* evolution and the CA mutant library approaches described here identified multiple Mx2 sensitivity determinants in the C-terminal domain. In principle, the CA surface these substitutions define is exposed to the host cytosol in the intact conical core, although this surface would likely be more accessible to interactions with host factors following disassembly/uncoating of the conical CA lattice. We also note that sensitivity to Mx2 could be altered by CA mutations through one or more of several mechanisms. Mutants could change the CA stability, could alter the way CA is recognized by host restriction factors (including Mx2 itself), or could alter the route by which HIV-1 accesses the nucleus. Each of these processes could change the sensitivity to Mx2. It seems unlikely that a single host factor would contact the HIV-1 CA in so many spatially distinct locations, and so it is possible that some of the Mx2 escape mutants described here confer resistance by altering the stability, structure, or nuclear import pathway. In this regard, it is interesting that Mx2 antiviral activity is sometimes, but not always, dependent on host cyclophilins. CsA is known to produce cell-type-dependent effects with respect to multiple phenotypes. Indeed, sensitivity to TRIM5α exhibits a variable dependence on host cyclophilins. Variable expression levels of CypA have been suggested as a possible explanation for the variable effects of CsA on HIV-1 infection and sensitivity to restriction factors (72).

As yet, we have been unable to identify any substitutions that confer efficient escape from Mx2 *in vitro* that also commonly occur in patient sequences. Moreover, all of the group M viruses tested thus far appear sensitive to inhibition by Mx2 (18–20). This includes "transmitted founder" viruses (18, 19) that have been proposed to be more resistant to inhibition by IFNs (73, 74). Thus, Mx2 might not exert a sufficiently strong pressure *in vivo* to drive the generation of CA escape mutants or maintain their continued presence. In light of this, sequences derived from cohorts of HIV-1-infected patients during acute infection or undergoing IFN-treatment might be required to observe frequent Mx2 escape mutants *in vivo*. Conversely, the extreme constraints placed upon CA to maintain replicative fitness (27) and evade both pattern recognition (75, 76) and immune responses (77–80) could simply result in Mx2-resistant viruses failing to thrive *in vivo*. Consistent with this idea, most substitutions conferring escape from Mx2 have substantially reduced fitness.

Further work is required to uncover the mechanistic basis of how Mx2 inhibits HIV-1 infection *in vitro* and to ascertain whether this inhibition occurs *in vivo*. Clearly, any inhibition that does occur in infected individuals is unable to tip the balance in favor of the host and clear HIV-1 infection. Thus, a complete understanding of this inhibitory interaction, which is perhaps underexploited in natural settings, could pave the way to harnessing Mx2 antiviral activity in a therapeutic context.

ACKNOWLEDGMENTS

We thank Hans-Georg Kräusslich, Theodora Hatziioannou, Alice Raymond, Andrew Shaw, Massimo Palmarini, Jim Neil, David Griffiths, Blue Tractor Software, and the Developmental Studies Hybridoma Bank at the University of Iowa for thoughtful advice and reagents.

This study was supported by an MRC Career Development award (to S.J.W.) and by the National Institutes of Health (R37AI64003 to P.D.B.).

REFERENCES

1. **Ho DD, Hartshorn KL, Rota TR, Andrews CA, Kaplan JC, Schooley RT, Hirsch MS.** 1985. Recombinant human interferon alfa-A suppresses HTLV-III replication in vitro. Lancet **i:**602–604.
2. **Asmuth DM, Murphy RL, Rosenkranz SL, Lertora JJ, Kottilil S, Cramer Y, Chan ES, Schooley RT, Rinaldo CR, Thielman N, Li XD, Wahl SM, Shore J, Janik J, Lempicki RA, Simpson Y, Pollard RB.** 2010. Safety, tolerability, and mechanisms of antiretroviral activity of pegylated interferon alfa-2a in HIV-1-monoinfected participants: a phase II clinical trial. J. Infect. Dis. **201:**1686–1696. http://dx.doi.org/10.1086/652420.
3. **Kirmaier A, Wu F, Newman RM, Hall LR, Morgan JS, O'Connor S, Marx PA, Meythaler M, Goldstein S, Buckler-White A, Kaur A, Hirsch VM, Johnson WE.** 2010. TRIM5 suppresses cross-species transmission of a primate immunodeficiency virus and selects for emergence of resistant variants in the new species. PLoS Biol. **8:**1–12. http://dx.doi.org/10.1371/journal.pbio.1000462.
4. **Liberatore RA, Bieniasz PD.** 2011. Tetherin is a key effector of the antiretroviral activity of type I interferon in vitro and in vivo. Proc. Natl. Acad. Sci. U. S. A. **108:**18097–18101. http://dx.doi.org/10.1073/pnas.1113694108.
5. **Okeoma CM, Lovsin N, Peterlin BM, Ross SR.** 2007. APOBEC3 inhibits mouse mammary tumour virus replication in vivo. Nature **445:**927–930. http://dx.doi.org/10.1038/nature05540.
6. **Hrecka K, Hao C, Gierszewska M, Swanson SK, Kesik-Brodacka M, Srivastava S, Florens L, Washburn MP, Skowronski J.** 2011. Vpx relieves inhibition of HIV-1 infection of macrophages mediated by the SAMHD1 protein. Nature **474:**658–661. http://dx.doi.org/10.1038/nature10195.
7. **Laguette N, Sobhian B, Casartelli N, Ringeard M, Chable-Bessia C, Segeral E, Yatim A, Emiliani S, Schwartz O, Benkirane M.** 2011. SAMHD1 is the dendritic- and myeloid-cell-specific HIV-1 restriction factor counteracted by Vpx. Nature **474:**654–657. http://dx.doi.org/10.1038/nature10117.
8. **Neil SJ, Zang T, Bieniasz PD.** 2008. Tetherin inhibits retrovirus release and is antagonized by HIV-1 Vpu. Nature **451:**425–430. http://dx.doi.org/10.1038/nature06553.
9. **Sheehy AM, Gaddis NC, Choi JD, Malim MH.** 2002. Isolation of a human gene that inhibits HIV-1 infection and is suppressed by the viral Vif protein. Nature **418:**646–650. http://dx.doi.org/10.1038/nature00939.
10. **Wilson SJ, Schoggins JW, Zang T, Kutluay SB, Jouvenet N, Alim MA, Bitzegeio J, Rice CM, Bieniasz PD.** 2012. Inhibition of HIV-1 particle assembly by 2′,3′-cyclic-nucleotide 3′-phosphodiesterase. Cell Host Microbe **12:**585–597. http://dx.doi.org/10.1016/j.chom.2012.08.012.
11. **Gao G, Guo X, Goff SP.** 2002. Inhibition of retroviral RNA production by ZAP, a CCCH-type zinc finger protein. Science **297:**1703–1706. http://dx.doi.org/10.1126/science.1074276.
12. **Furtak V, Mulky A, Rawlings SA, Kozhaya L, Lee K, Kewalramani VN, Unutmaz D.** 2010. Perturbation of the P-body component Mov10 inhibits HIV-1 infectivity. PLoS One **5:**e9081. http://dx.doi.org/10.1371/journal.pone.0009081.
13. **Goujon C, Schaller T, Galao RP, Amie SM, Kim B, Olivieri K, Neil SJ,**

Malim MH. 2013. Evidence for IFNα-induced, SAMHD1-independent inhibitors of early HIV-1 infection. Retrovirology **10:**23. http://dx.doi.org/10.1186/1742-4690-10-23.
14. **Lindenmann J.** 1962. Resistance of mice to mouse-adapted influenza A virus. Virology **16:**203–204. http://dx.doi.org/10.1016/0042-6822(62)90297-0.
15. **Staeheli P, Haller O, Boll Lindenmann WJ, Weissmann C.** 1986. Mx protein: constitutive expression in 3T3 cells transformed with cloned Mx cDNA confers selective resistance to influenza virus. Cell **44:**147–158. http://dx.doi.org/10.1016/0092-8674(86)90493-9.
16. **King MC, Raposo G, Lemmon MA.** 2004. Inhibition of nuclear import and cell-cycle progression by mutated forms of the dynamin-like GTPase MxB. Proc. Natl. Acad. Sci. U. S. A. **101:**8957–8962. http://dx.doi.org/10.1073/pnas.0403167101.
17. **Schoggins JW, Wilson SJ, Panis M, Murphy MY, Jones CT, Bieniasz P, Rice CM.** 2011. A diverse range of gene products are effectors of the type I interferon antiviral response. Nature **472:**481–485. http://dx.doi.org/10.1038/nature09907.
18. **Kane M, Yadav SS, Bitzegeio J, Kutluay SB, Zang T, Wilson SJ, Schoggins JW, Rice CM, Yamashita M, Hatziioannou T, Bieniasz PD.** 2013. MX2 is an interferon-induced inhibitor of HIV-1 infection. Nature **502:**563–566. http://dx.doi.org/10.1038/nature12653.
19. **Goujon C, Moncorge O, Bauby H, Doyle T, Ward CC, Schaller T, Hue S, Barclay WS, Schulz R, Malim MH.** 2013. Human MX2 is an interferon-induced post-entry inhibitor of HIV-1 infection. Nature **502:**559–562. http://dx.doi.org/10.1038/nature12542.
20. **Liu Z, Pan Q, Ding S, Qian J, Xu F, Zhou J, Cen S, Guo F, Liang C.** 2013. The interferon-inducible MxB protein inhibits HIV-1 infection. Cell Host Microbe **14:**398–410. http://dx.doi.org/10.1016/j.chom.2013.08.015.
21. **Wiederschain D, Wee S, Chen L, Loo A, Yang G, Huang A, Chen Y, Caponigro G, Yao YM, Lengauer C, Sellers WR, Benson JD.** 2009. Single-vector inducible lentiviral RNAi system for oncology target validation. Cell Cycle **8:**498–504. http://dx.doi.org/10.4161/cc.8.3.7701.
22. **Everett RD, Parsy ML, Orr A.** 2009. Analysis of the functions of herpes simplex virus type 1 regulatory protein ICP0 that are critical for lytic infection and derepression of quiescent viral genomes. J. Virol. **83:**4963–4977. http://dx.doi.org/10.1128/JVI.02593-08.
23. **Arnaud F, Black SG, Murphy L, Griffiths DJ, Neil SJ, Spencer TE, Palmarini M.** 2010. Interplay between ovine bone marrow stromal cell antigen 2/tetherin and endogenous retroviruses. J. Virol. **84:**4415–4425. http://dx.doi.org/10.1128/JVI.00029-10.
24. **Tebit DM, Zekeng L, Kaptue L, Gurtler L, Fackler OT, Keppler OT, Herchenroder O, Krausslich HG.** 2004. Construction and characterization of an HIV-1 group O infectious molecular clone and analysis of vpr- and nef-negative derivatives. Virology **326:**329–339. http://dx.doi.org/10.1016/j.virol.2004.05.027.
25. **Wilson SJ, Webb BL, Ylinen LM, Verschoor E, Heeney JL, Towers GJ.** 2008. Independent evolution of an antiviral TRIMCyp in rhesus macaques. Proc. Natl. Acad. Sci. U. S. A. **105:**3557–3562. http://dx.doi.org/10.1073/pnas.0709003105.
26. **Virgen CA, Kratovac Z, Bieniasz PD, Hatziioannou T.** 2008. Independent genesis of chimeric TRIM5-cyclophilin proteins in two primate species. Proc. Natl. Acad. Sci. U. S. A. **105:**3563–3568. http://dx.doi.org/10.1073/pnas.0709258105.
27. **Rihn SJ, Wilson SJ, Loman NJ, Alim M, Bakker SE, Bhella D, Gifford RJ, Rixon FJ, Bieniasz PD.** 2013. Extreme genetic fragility of the HIV-1 capsid. PLoS Pathog. **9:**e1003461. http://dx.doi.org/10.1371/journal.ppat.1003461.
28. **Soll SJ, Wilson SJ, Kutluay SB, Hatziioannou T, Bieniasz PD.** 2013. Assisted evolution enables HIV-1 to overcome a high TRIM5α-imposed genetic barrier to rhesus macaque tropism. PLoS Pathog. **9:**e1003667. http://dx.doi.org/10.1371/journal.ppat.1003667.
29. **Sambrook J, Fritsch EF, Maniatis T.** 1989. Molecular cloning, vol 2. Cold Spring Harbor Laboratory Press, New York, NY.
30. **Jouvenet N, Neil SJ, Bess C, Johnson MC, Virgen CA, Simon SM, Bieniasz PD.** 2006. Plasma membrane is the site of productive HIV-1 particle assembly. PLoS Biol. **4:**e435. http://dx.doi.org/10.1371/journal.pbio.0040435.
31. **Pornillos O, Ganser-Pornillos BK, Kelly BN, Hua Y, Whitby FG, Stout CD, Sundquist WI, Hill CP, Yeager M.** 2009. X-ray structures of the hexameric building block of the HIV capsid. Cell **137:**1282–1292. http://dx.doi.org/10.1016/j.cell.2009.04.063.
32. **Sievers F, Wilm A, Dineen D, Gibson TJ, Karplus K, Li W, Lopez R, McWilliam H, Remmert M, Soding J, Thompson JD, Higgins DG.** 2011. Fast, scalable generation of high-quality protein multiple sequence alignments using Clustal Omega. Mol. Syst. Biol. **7:**539. http://dx.doi.org/10.1038/msb.2011.75.
33. **Suyama M, Torrents D, Bork P.** 2006. PAL2NAL: robust conversion of protein sequence alignments into the corresponding codon alignments. Nucleic Acids Res. **34:**W609–W612. http://dx.doi.org/10.1093/nar/gkl315.
34. **Darriba D, Taboada GL, Doallo R, Posada D.** 2012. jModelTest 2: more models, new heuristics and parallel computing. Nat. Methods **9:**772. http://dx.doi.org/10.1038/nmeth.2111.
35. **Guindon S, Gascuel O.** 2003. A simple, fast, and accurate algorithm to estimate large phylogenies by maximum likelihood. Syst. Biol. **52:**696–704. http://dx.doi.org/10.1080/10635150390235520.
36. **Delport W, Poon AF, Frost SD, Kosakovsky Pond SL.** 2010. Datamonkey 2010: a suite of phylogenetic analysis tools for evolutionary biology. Bioinformatics **26:**2455–2457. http://dx.doi.org/10.1093/bioinformatics/btq429.
37. **Yang Z.** 1997. PAML: a program package for phylogenetic analysis by maximum likelihood. Comput. Appl. Biosci. (Camb.) **13:**555–556.
38. **Stamatakis A.** 2006. RAxML-VI-HPC: maximum likelihood-based phylogenetic analyses with thousands of taxa and mixed models. Bioinformatics **22:**2688–2690. http://dx.doi.org/10.1093/bioinformatics/btl446.
39. **Hatziioannou T, Perez-Caballero D, Yang A, Cowan S, Bieniasz PD.** 2004. Retrovirus resistance factors Ref1 and Lv1 are species-specific variants of TRIM5α. Proc. Natl. Acad. Sci. U. S. A. **101:**10774–10779. http://dx.doi.org/10.1073/pnas.0402361101.
40. **Ohkura S, Goldstone DC, Yap MW, Holden-Dye K, Taylor IA, Stoye JP.** 2011. Novel escape mutants suggest an extensive TRIM5α binding site spanning the entire outer surface of the murine leukemia virus capsid protein. PLoS Pathog. **7:**e1002011. http://dx.doi.org/10.1371/journal.ppat.1002011.
41. **Sebastian S, Luban J.** 2005. TRIM5α selectively binds a restriction-sensitive retroviral capsid. Retrovirology **2:**40. http://dx.doi.org/10.1186/1742-4690-2-40.
42. **Sawyer SL, Wu LI, Emerman M, Malik HS.** 2005. Positive selection of primate TRIM5α identifies a critical species-specific retroviral restriction domain. Proc. Natl. Acad. Sci. U. S. A. **102:**2832–2837. http://dx.doi.org/10.1073/pnas.0409853102.
43. **Zhang F, Wilson SJ, Landford WC, Virgen B, Gregory D, Johnson MC, Munch J, Kirchhoff F, Bieniasz PD, Hatziioannou T.** 2009. Nef proteins from simian immunodeficiency viruses are tetherin antagonists. Cell Host Microbe **6:**54–67. http://dx.doi.org/10.1016/j.chom.2009.05.008.
44. **Jia B, Serra-Moreno R, Neidermyer W, Rahmberg A, Mackey J, Fofana IB, Johnson WE, Westmoreland S, Evans DT.** 2009. Species-specific activity of SIV Nef and HIV-1 Vpu in overcoming restriction by tetherin/BST2. PLoS pathogens **5:**e1000429. http://dx.doi.org/10.1371/journal.ppat.1000429.
45. **Zhang F, Landford WN, Ng M, McNatt MW, Bieniasz PD, Hatziioannou T.** 2011. SIV Nef proteins recruit the AP-2 complex to antagonize Tetherin and facilitate virion release. PLoS Pathog. **7:**e1002039. http://dx.doi.org/10.1371/journal.ppat.1002039.
46. **Serra-Moreno R, Zimmermann K, Stern LJ, Evans DT.** 2013. Tetherin/BST-2 antagonism by Nef depends on a direct physical interaction between Nef and tetherin, and on clathrin-mediated endocytosis. PLoS Pathog. **9:**e1003487. http://dx.doi.org/10.1371/journal.ppat.1003487.
47. **Ko JH, Jin HK, Asano A, Takada A, Ninomiya A, Kida H, Hokiyama H, Ohara M, Tsuzuki M, Nishibori M, Mizutani M, Watanabe T.** 2002. Polymorphisms and the differential antiviral activity of the chicken Mx gene. Genome Res. **12:**595–601. http://dx.doi.org/10.1101/gr.210702.
48. **Larsen R, Rokenes TP, Robertsen B.** 2004. Inhibition of infectious pancreatic necrosis virus replication by Atlantic salmon Mx1 protein. J. Virol. **78:**7938–7944. http://dx.doi.org/10.1128/JVI.78.15.7938-7944.2004.
49. **Newman RM, Hall L, Connole M, Chen GL, Sato S, Yuste E, Diehl W, Hunter E, Kaur A, Miller GM, Johnson WE.** 2006. Balancing selection and the evolution of functional polymorphism in Old World monkey TRIM5α. Proc. Natl. Acad. Sci. U. S. A. **103:**19134–19139. http://dx.doi.org/10.1073/pnas.0605838103.
50. **Song C, Hunter E.** 2003. Variable sensitivity to substitutions in the N-terminal heptad repeat of Mason-Pfizer monkey virus transmembrane protein. J. Virol. **77:**7779–7785. http://dx.doi.org/10.1128/JVI.77.14.7779-7785.2003.
51. **Lee YN, Bieniasz PD.** 2007. Reconstitution of an infectious human en-

dogenous retrovirus. PLoS Pathog. **3:**e10. http://dx.doi.org/10.1371/journal.ppat.0030010.
52. **Melen K, Keskinen P, Ronni T, Sareneva T, Lounatmaa K, Julkunen I.** 1996. Human MxB protein, an interferon-alpha-inducible GTPase, contains a nuclear targeting signal and is localized in the heterochromatin region beneath the nuclear envelope. J. Biol. Chem. **271:**23478–23486. http://dx.doi.org/10.1074/jbc.271.38.23478.
53. **Ptak RG, Gallay PA, Jochmans D, Halestrap AP, Ruegg UT, Pallansch LA, Bobardt MD, de Bethune MP, Neyts J, De Clercq E, Dumont JM, Scalfaro P, Besseghir K, Wenger RM, Rosenwirth B.** 2008. Inhibition of human immunodeficiency virus type 1 replication in human cells by Debio-025, a novel cyclophilin binding agent. Antimicrob. Agents Chemother. **52:**1302–1317. http://dx.doi.org/10.1128/AAC.01324-07.
54. **Newman RM, Hall L, Kirmaier A, Pozzi LA, Pery E, Farzan M, O'Neil SP, Johnson W.** 2008. Evolution of a TRIM5-CypA splice isoform in old world monkeys. PLoS Pathog. **4:**e1000003. http://dx.doi.org/10.1371/journal.ppat.1000003.
55. **Yamashita M, Perez O, Hope TJ, Emerman M.** 2007. Evidence for direct involvement of the capsid protein in HIV infection of nondividing cells. PLoS Pathog. **3:**1502–1510. http://dx.doi.org/10.1371/journal.ppat.0030156.
56. **McCarthy KR, Schmidt AG, Kirmaier A, Wyand AL, Newman RM, Johnson WE.** 2013. Gain-of-sensitivity mutations in a Trim5-resistant primary isolate of pathogenic SIV identify two independent conserved determinants of Trim5α specificity. PLoS Pathog. **9:**e1003352. http://dx.doi.org/10.1371/journal.ppat.1003352.
57. **Zhao G, Perilla JR, Yufenyuy EL, Meng X, Chen B, Ning J, Ahn J, Gronenborn AM, Schulten K, Aiken C, Zhang P.** 2013. Mature HIV-1 capsid structure by cryo-electron microscopy and all-atom molecular dynamics. Nature **497:**643–646. http://dx.doi.org/10.1038/nature12162.
58. **Forshey BM, von Schwedler U, Sundquist WI, Aiken C.** 2002. Formation of a human immunodeficiency virus type 1 core of optimal stability is crucial for viral replication. J. Virol. **76:**5667–5677. http://dx.doi.org/10.1128/JVI.76.11.5667-5677.2002.
59. **Lee K, Ambrose Z, Martin TD, Oztop I, Mulky A, Julias JG, Vandegraaff N, Baumann JG, Wang R, Yuen W, Takemura T, Shelton K, Taniuchi I, Li Y, Sodroski J, Littman DR, Coffin JM, Hughes SH, Unutmaz D, Engelman A, KewalRamani VN.** 2010. Flexible use of nuclear import pathways by HIV-1. Cell Host Microbe **7:**221–233. http://dx.doi.org/10.1016/j.chom.2010.02.007.
60. **Krishnan L, Matreyek KA, Oztop I, Lee K, Tipper CH, Li X, Dar MJ, Kewalramani VN, Engelman A.** 2010. The requirement for cellular transportin 3 (TNPO3 or TRN-SR2) during infection maps to human immunodeficiency virus type 1 capsid and not integrase. J. Virol. **84:**397–406. http://dx.doi.org/10.1128/JVI.01899-09.
61. **Schaller T, Ocwieja KE, Rasaiyaah J, Price AJ, Brady TL, Roth SL, Hue S, Fletcher AJ, Lee K, KewalRamani VN, Noursadeghi M, Jenner RG, James LC, Bushman FD, Towers GJ.** 2011. HIV-1 capsid-cyclophilin interactions determine nuclear import pathway, integration targeting, and replication efficiency. PLoS Pathog. **7:**e1002439. http://dx.doi.org/10.1371/journal.ppat.1002439.
62. **Mitchell PS, Patzina C, Emerman M, Haller O, Malik HS, Kochs G.** 2012. Evolution-guided identification of antiviral specificity determinants in the broadly acting interferon-induced innate immunity factor MxA. Cell Host Microbe **12:**598–604. http://dx.doi.org/10.1016/j.chom.2012.09.005.
63. **McNatt MW, Zang T, Hatziioannou T, Bartlett M, Fofana IB, Johnson WE, Neil SJ, Bieniasz PD.** 2009. Species-specific activity of HIV-1 Vpu and positive selection of tetherin transmembrane domain variants. PLoS Pathog. **5:**e1000300. http://dx.doi.org/10.1371/journal.ppat.1000300.
64. **Turan K, Mibayashi M, Sugiyama K, Saito S, Numajiri A, Nagata K.** 2004. Nuclear MxA proteins form a complex with influenza virus NP and inhibit the transcription of the engineered influenza virus genome. Nucleic Acids Res. **32:**643–652. http://dx.doi.org/10.1093/nar/gkh192.
65. **Kochs G, Haller O.** 1999. GTP-bound human MxA protein interacts with the nucleocapsids of Thogoto virus (*Orthomyxoviridae*). J. Biol. Chem. **274:**4370–4376. http://dx.doi.org/10.1074/jbc.274.7.4370.
66. **Gao S, von der Malsburg A, Paeschke S, Behlke J, Haller O, Kochs G, Daumke O.** 2010. Structural basis of oligomerization in the stalk region of dynamin-like MxA. Nature **465:**502–506. http://dx.doi.org/10.1038/nature08972.
67. **Haller O.** 2013. Dynamins are forever: MxB inhibits HIV-1. Cell Host Microbe **14:**371–373. http://dx.doi.org/10.1016/j.chom.2013.10.002.
68. **Ganser-Pornillos BK, Chandrasekaran V, Pornillos O, Sodroski JG, Sundquist WI, Yeager M.** 2011. Hexagonal assembly of a restricting TRIM5α protein. Proc. Natl. Acad. Sci. U. S. A. **108:**534–539. http://dx.doi.org/10.1073/pnas.1013426108.
69. **Yang H, Ji X, Zhao G, Ning J, Zhao Q, Aiken C, Gronenborn AM, Zhang P, Xiong Y.** 2012. Structural insight into HIV-1 capsid recognition by rhesus TRIM5α. Proc. Natl. Acad. Sci. U. S. A. **109:**18372–18377. http://dx.doi.org/10.1073/pnas.1210903109.
70. **Price AJ, Fletcher AJ, Schaller T, Elliott T, Lee K, KewalRamani VN, Chin JW, Towers GJ, James LC.** 2012. CPSF6 defines a conserved capsid interface that modulates HIV-1 replication. PLoS Pathog. **8:**e1002896. http://dx.doi.org/10.1371/journal.ppat.1002896.
71. **Matreyek KA, Yucel SS, Li X, Engelman A.** 2013. Nucleoporin NUP153 phenylalanine-glycine motifs engage a common binding pocket within the HIV-1 capsid protein to mediate lentiviral infectivity. PLoS Pathog. **9:**e1003693. http://dx.doi.org/10.1371/journal.ppat.1003693.
72. **Ylinen LM, Schaller T, Price A, Fletcher AJ, Noursadeghi M, James LC, Towers GJ.** 2009. Cyclophilin A levels dictate infection efficiency of human immunodeficiency virus type 1 capsid escape mutants A92E and G94D. J. Virol. **83:**2044–2047. http://dx.doi.org/10.1128/JVI.01876-08.
73. **Fenton-May AE, Dibben O, Emmerich T, Ding H, Pfafferott K, Aasa-Chapman MM, Pellegrino P, Williams I, Cohen MS, Gao F, Shaw GM, Hahn BH, Ochsenbauer C, Kappes JC, Borrow P.** 2013. Relative resistance of HIV-1 founder viruses to control by interferon-alpha. Retrovirology **10:**146. http://dx.doi.org/10.1186/1742-4690-10-146.
74. **Parrish NF, Gao F, Li H, Giorgi EE, Barbian HJ, Parrish EH, Zajic L, Iyer SS, Decker JM, Kumar A, Hora B, Berg A, Cai F, Hopper J, Denny TN, Ding H, Ochsenbauer C, Kappes JC, Galimidi RP, West AP, Jr, Bjorkman PJ, Wilen CB, Doms RW, O'Brien M, Bhardwaj N, Borrow P, Haynes BF, Muldoon M, Theiler JP, Korber B, Shaw GM, Hahn BH.** 2013. Phenotypic properties of transmitted founder HIV-1. Proc. Natl. Acad. Sci. U. S. A. **110:**6626–6633. http://dx.doi.org/10.1073/pnas.1304288110.
75. **Manel N, Hogstad B, Wang Y, Levy DE, Unutmaz D, Littman DR.** 2010. A cryptic sensor for HIV-1 activates antiviral innate immunity in dendritic cells. Nature **467:**214–217. http://dx.doi.org/10.1038/nature09337.
76. **Rasaiyaah J, Tan CP, Fletcher AJ, Price AJ, Blondeau C, Hilditch L, Jacques DA, Selwood DL, James LC, Noursadeghi M, Towers GJ.** 2013. HIV-1 evades innate immune recognition through specific cofactor recruitment. Nature **503:**402–405. http://dx.doi.org/10.1038/nature12769.
77. **Borrow P, Lewicki H, Hahn BH, Shaw GM, Oldstone MB.** 1994. Virus-specific $CD8^+$ cytotoxic T-lymphocyte activity associated with control of viremia in primary human immunodeficiency virus type 1 infection. J. Virol. **68:**6103–6110.
78. **Dahirel V, Shekhar K, Pereyra F, Miura T, Artyomov M, Talsania S, Allen TM, Altfeld M, Carrington M, Irvine DJ, Walker BD, Chakraborty AK.** 2011. Coordinate linkage of HIV evolution reveals regions of immunological vulnerability. Proc. Natl. Acad. Sci. U. S. A. **108:**11530–11535. http://dx.doi.org/10.1073/pnas.1105315108.
79. **Brockman MA, Brumme ZL, Brumme CJ, Miura T, Sela J, Rosato PC, Kadie CM, Carlson JM, Markle TJ, Streeck H, Kelleher AD, Markowitz M, Jessen H, Rosenberg E, Altfeld M, Harrigan PR, Heckerman D, Walker BD, Allen TM.** 2010. Early selection in Gag by protective HLA alleles contributes to reduced HIV-1 replication capacity that may be largely compensated for in chronic infection. J. Virol. **84:**11937–11949. http://dx.doi.org/10.1128/JVI.01086-10.
80. **International HIVCS, Pereyra F, Jia X, McLaren PJ, Telenti A, de Bakker PI, Walker BD, Ripke S, Brumme CJ, Pulit SL, Carrington M, Kadie CM, Carlson JM, Heckerman D, Graham RR, Plenge RM, Deeks SG, Gianniny L, Crawford G, Sullivan J, Gonzalez E, Davies L, Camargo A, Moore JM, Beattie N, Gupta S, Crenshaw A, Burtt NP, Guiducci C, Gupta N, Gao X, Qi Y, Yuki Y, Piechocka-Trocha A, Cutrell E, Rosenberg R, Moss KL, Lemay P, O'Leary J, Schaefer T, Verma P, Toth I, Block B, Baker B, Rothchild A, Lian J, Proudfoot J, Alvino DM, et al.** 2010. The major genetic determinants of HIV-1 control affect HLA class I peptide presentation. Science **330:**1551–1557. http://dx.doi.org/10.1126/science.1195271.
81. **Demaison C, Parsley K, Brouns G, Scherr M, Battmer K, Kinnon C, Grez M, Thrasher AJ.** 2002. High-level transduction and gene expression in hematopoietic repopulating cells using a human immunodeficiency virus type 1-based lentiviral vector containing an internal spleen focus forming virus promoter. Hum. Gene Ther. **13:**803–813. http://dx.doi.org/10.1089/10430340252898984.
82. **Saenz DT, Poeschla EM.** 2004. FIV: from lentivirus to lentivector. J. Gene Med. **6**(Suppl 1)**:**S95–S104.